PERGAMON

International Journal of Heat and Mass Transfer 42 (1999) 1429–1456

International Journal of HEAT and MASS TRANSFER

Ultra-high critical heat flux (CHF) for subcooled water flow boiling—II: high-CHF database and design equations

David D. Hall, Issam Mudawar*

Boiling and Two-Phase Flow Laboratory, School of Mechanical Engineering, Purdue University, West Lafayette, IN 47907, U.S.A.

Received 28 October 1997; in final form 27 July 1998

Abstract

A high-CHF (critical heat flux) database for subcooled flow boiling of water in tubes was compiled from the world literature. The bulk of the database is for high mass velocity flow ($G \geqslant 5000$ kg m^{-2} s^{-1}) in small diameter tubes ($D \leqslant 3$ mm). Over half of the 1596 valid data points in the database had CHF values in excess of 25 MW m^{-2}. The database included the highest CHF for uniform heating ever reported in the literature, 276 MW m^{-2}, which was obtained in Part I of the present study. A pressure drop model applicable to subcooled flow boiling in tubes with inlet and outlet plenums was developed in order to determine the pressure at the end of the heated length where burnout (CHF) was observed. The pressure at this location is often significantly different from that measured downstream in the outlet plenum. A subcooled high-CHF correlation superior to previously published correlations was systematically developed using data only from the authors' institution and Kiev Polytechnic Institute, Kiev, Ukraine. The correlation was validated with data covering a broad range of pressures (from atmospheric to near the critical point) and mass velocities (1500–134 000 kg m^{-2} s^{-1}) which are required in the cooling of high-heat-flux components, such as those in fusion reactors. Although it was developed by examining the parametric trends exhibited by a small fraction of the database, the correlation had a root-mean-square error of 19.5% for the entire database, lowest among the correlations tested. In sharp contrast to other correlations, this new, dimensionless CHF correlation consisted of a single equation having only five adjustable constants.

Nomenclature

A cross-sectional area
A_c cross-sectional flow area at vena contracta
a_j constant defined in equation (35), $j = 1, 2, 3,$ or 4
$a_{j'}$ constant defined in equation (40), $j = 1$ or 2
b_j constant defined in equation (35), $j = 1, 2, 3,$ or 4
Bo boiling number, q_m/Gh_{fg}
C constant defined in equations (3) and (4)
C_c jet contraction ratio defined by equation (14)
C_j constant defined in equations (7) and (8), $j = 1, 2, \ldots, 11$
c_j constant defined in equations (30) and (31), $j = 1$ or 2
D inside diameter of tube
e internal energy
E kinetic energy correction factor
f fully developed turbulent flow (Fanning) friction factor
f_{app} mean apparent (Fanning) friction factor defined in equation (11)
f_j function of density ratio defined in Fig. 6(a) and (b) and equations (33)–(35), $j = 1, 2, 3,$ or 4
fn( ) function of ( )
G mass velocity
h enthalpy of fluid
h_f enthalpy of saturated liquid
h_{fg} latent heat of vaporization
Δh_{sub} liquid subcooling, $h_f - h$, with enthalpy of saturated liquid evaluated at pressure associated with the CHF data point (usually outlet pressure)
K irreversible loss coefficient
L heated length of tube
L_t total length of tube
L_{uh} unheated length of tube upstream or downstream of heated section

*Corresponding author. Fax: 001 765 494 0539; e-mail: mudawar@ecu.purdue.edu

0017–9310/98/$ - see front matter
PII: S0017–9310(98)00242–7

M momentum correction factor
N number of CHF data points
P pressure
ΔP pressure drop
q heat flux defined using tube inside area
q_m critical heat flux (CHF) defined using tube inside area
Re_D Reynolds number, GD/μ_f
T temperature
T_i bulk liquid temperature at inlet
T_o bulk liquid temperature at outlet (defined only if $x_o < 0$)
ΔT_{sub} liquid subcooling, $T_{sat} - T$, with saturation temperature evaluated at pressure associated with the CHF data point (usually outlet pressure)
u axial velocity
U mean axial velocity across flow area
We_D Weber number, $G^2D/\rho_f\sigma$
x thermodynamic equilibrium quality, $(h-h_f)/h_{fg}$, with saturated thermophysical properties evaluated at pressure associated with the CHF data point (usually outlet pressure) unless specifically stated otherwise
$x_{i,*}$ pseudo-inlet quality, $(h_i-h_{f,o})/h_{fg,o}$, with saturated thermophysical properties evaluated at outlet pressure
z axial location.

Greek symbols
β ratio of tube flow area to plenum flow area
μ dynamic viscosity
ρ density
σ surface tension
Ψ constant defined in equation (6).

Subscripts
1 at station 1 downstream of vena contracta (see Fig. 1(a))
2 at station 2 at test section exit (see Fig. 1(a))
c contraction; at vena contracta (see Fig. 1(a))
e expansion
f liquid; friction
g vapor
i inlet; beginning of heated length (see Fig. 1(b))
ideal ideal, frictionless flow
max maximum
meas measured
o outlet; end of heated length (see Fig. 1(b))
p plenum (see Fig. 1(a) and (b))
pred predicted
sat saturated conditions
sub subcooled conditions
tp triple-point
uh unheated section.

1. Introduction

Critical heat flux (CHF) refers to the heat transfer limit causing a sudden rise in surface temperature and possible catastrophic failure of a device in which evaporation or boiling is occurring. The nuclear power industry has been at the forefront in research efforts aimed at understanding pool and flow boiling CHF, particularly in relation to the design and safe-operation of water-cooled nuclear reactors. Insufficient cooling during an over-power transient or a loss-of-coolant accident may cause CHF leading to a core meltdown and subsequent release of radioactive material into the environment. Recently, CHF has become increasingly important in many additional applications, including, for example, particle accelerator targets, high-power X-ray devices, rocket nozzles, cryogenic cooling systems in satellites and compact two-phase heat exchangers in aerospace systems (avionics) and supercomputers.

The cooling of fusion reactor components will require high mass velocity, subcooled flow boiling of water in small diameter channels to maintain the extreme operating conditions safely below CHF. The term 'burnout' is often used in this high heat flux application since physical destruction of the system will occur as a result of a large wall temperature excursion at CHF. The mass velocity, pressure, and enthalpy of the flow at the burnout location as well as the hydraulic diameter have a pronounced effect on CHF and, consequently, accurate knowledge of these parameters is of paramount importance in predicting CHF. The objectives of the present study are the following: (1) compile subcooled high-CHF data for water flow in a uniformly heated tube, (2) determine the accuracy of existing subcooled CHF correlations which were developed using data similar to that compiled in this study, (3) develop a pressure drop model for determining the local pressure at burnout, and (4) develop a simple, dimensionless, subcooled CHF correlation which is superior in accuracy to existing correlations.

2. High-CHF database

The literature from the past fifty years was thoroughly examined for subcooled high-CHF data obtained with water flow in a uniformly heated tube. Table 1 lists those studies [1–23] found to contain at least one data point having a CHF value in excess of 25 MW m^{-2}. Both vertical upflow and horizontal flow CHF data were compiled since CHF at high mass velocities is unaffected by flow orientation. Some data were excluded from further analysis: data identified by the original authors as unreliable (e.g., premature CHF or inaccurate measurements) [25], duplicate data identified by the present authors [25], data which violated an energy balance (see discussion below), data which inexplicably yielded an inlet temperature less than 0°C, and data corresponding to saturated conditions at CHF (i.e., positive outlet quality). Table 2 lists the parametric ranges associated with the remaining, valid data. Over 850 of the 1596 valid data

Table 1
Studies of subcooled water flow boiling in uniformly heated tubes with CHF values in excess of 25 MW m^{-2}

Reference	Total CHF data points	Unreliable data	Duplicate data	Energy balance violation	$T_i \leqslant 0°C$	$x_o \geqslant 0$	Acceptable subcooled CHF data
Gambill and Greene [1]	7	0	0	—	0	0	7
Gambill et al. [2]	24	0	0	0	0	0	24
Ornatskii and Kichigin [3]	224	0	0	—	2	0	222
Bergles and Rohsenow [4]	51	2	0	—	0	3	46
Ornatskii and Kichigin [5]	111	0	0	—	1	0	110
Bergles [6]†	69	0	0	—	0	13	56
Ornatskii [7]	69	0	0	—	2	0	67
Mayersak et al. [8]	1	0	0	—	0	0	1
Ornatskii and Vinyarskii [9]	109	0	0	—	13	0	96
Skinner and Loosmore [10]	111	12	0	—	1	0	98
Zeigarnik et al. [11]	28	0	0	—	8	0	20
Nariai et al. [12]‡	95	0	0	0	0	3	92
Boyd [13]	5	0	0	0	0	0	5
Boyd [14]	5	0	0	—	0	0	5
Inasaka and Nariai [15]	29	0	0	0	0	0	29
Celata et al. [16]§	60	0	0	—	0	0	60
Celata et al. [17]	43	0	0	—	0	0	43
Celata et al. [18]	78	0	0	—	0	0	78
Celata and Mariani [19]	87	0	0	—	0	0	87
Gaspari and Cattadori [20]	33	0	0	—	0	0	33
Vandervort et al. [21]	255	45	8	—	0	0	202
Celata [22]	41	0	0	—	0	0	41
Part I [23] of present study	174	0	0	0	0	0	174
High-CHF database	1709	59	8	0	27	19	1596

† Data obtained from Skinner and Loosmore [10]; ‡ data obtained from Inasaka [24]; § data obtained from Celata and Mariani [19].
Reference—publication by the authors who obtained the CHF data. If CHF data were not tabulated in this reference, then one of the symbols above identifies the source of the data.
Total CHF data points—CHF data obtained with water flow in a uniformly heated tube.
Unreliable data—CHF data identified as invalid by either the original authors or authors of the present study (see Ref. [25] for details).
Duplicate data—CHF data appeared in another reference (see Ref. [25] for details).
Energy balance violation—outlet quality tabulated in the reference differed by more than 0.05 (0.10 if pressure was greater than 75% of critical pressure) from outlet quality calculated by the authors of the present study using the tabulated inlet condition and an energy balance. A dash indicates that inlet and outlet conditions were not both tabulated and, thus, data were not verifiable using an energy balance. A zero indicates that all data satisfied an energy balance.
$T_i \leqslant 0°C$—inlet temperature calculated using the tabulated outlet subcooling and an energy balance was less than 0°C.
$x_o \geqslant 0$—outlet quality calculated using the tabulated inlet condition and an energy balance was positive.
Acceptable subcooled CHF data—total number of CHF data points minus the number of invalid and saturated CHF data indicated in the preceding columns.

points in the database had CHF values in excess of 25 MW m^{-2}. The highest CHF ever measured for a uniformly heated tube (276 MW m^{-2}) was obtained in Part I [23] of the present study at the following test conditions: $D = 0.406$ mm, $L = 5.8$ mm ($L/D = 14.3$), $G = 120\,000$ kg m^{-2} s^{-1}, $P = 27$ bars, $x_o = -0.40$ and $\Delta T_{sub,o} = 169°C$. This surpassed the prior CHF record of 228 MW m^{-2} achieved by Ornatskii and Vinyarskii [9].

The first law of thermodynamics requires that the energy content of a unit mass of fluid at the tube outlet (outlet enthalpy) is equal to the energy content at the inlet (inlet enthalpy) plus the energy added as the unit mass passes through the heated tube (heat input divided by mass flow rate),

$$h_o = h_i + 4\frac{L}{D}\frac{q_m}{G}. \quad (1)$$

CHF data from each reference listed in Table 1 were tabulated in a spreadsheet. If the tabulated inlet condition was inlet quality or subcooling, then the inlet temperature was calculated using equations for saturation temperature, saturated liquid enthalpy, and latent heat of vaporization given in ref. [26]. The enthalpy of subcooled liquid was approximated by the saturated liquid enthalpy

Table 2
Parametric ranges of the acceptable subcooled CHF data

Reference	Acceptable CHF data	Test section					$G\times10^{-3}$ [kg m^{-2} s^{-1}]	P_o [bars]	Inlet condition		Outlet condition		CHF
		Orientation material	Unheated entrance region	Unheated exit region	D [mm]	L/D			$\Delta T_{sub,i}$ [°C]	x_i	$\Delta T_{sub,o}$ [°C]	x_o	$q_m\times10^{-6}$ [W m^{-2}]
Gambill and Greene [1]	7	Horizontal type "A" Ni	$L_{uh}/D = 10$	Unknown	7.7	6	13	1	64	−0.18	57	−0.16	16
					7.7	20	26	1	95	−0.12	88	−0.11	33
Gambill et al. [2]	24	Horizontal type "A" Ni	$L_{uh}/D \approx 40$	Unknown	3.2	7	7	0.7	76	−0.28	10	−0.24	7
					7.7	88	53	5	141	−0.14	122	−0.02	54
Ornatskii and Kichigin [3]	222	Vertical Cu alloy	$L_{uh}/D = 27$	L_{uh}/D not specified	2.0	20	5	10	15	−0.80	1	−0.65	6
					2.0	20	30	74	263	−0.04	212	0.00	71
Bergles and Rohsenow [4]	46	Horizontal SS-304	$L_{uh}/D = 17$ (0, 4, 7, 9)	Unknown	0.6	5	3	2	38	−0.22	1	−0.08	6
					4.6	50	6	2	115	−0.07	44	0.00	25
Ornatskii and Kichigin [5]	110	Vertical Cu alloy	$L_{uh}/D = 27$	L_{uh}/D not specified	2.0	20	5	98	13	−1.54	6	−1.19	8
					2.0	20	30	147	333	−0.08	250	−0.03	72
Bergles [6]†	56	Horizontal SS	$L_{uh}/D = 17$ (0, 13)	Unknown	1.2	13	1.5	1	38	−0.22	3	−0.14	5
					6.1	26	24	6	113	−0.07	71	−0.01	45
Ornatskii [7]	67	Vertical Cu alloy	$L_{uh}/D = 27$	L_{uh}/D not specified	2.0	20	5	172	22	−2.47	4	−2.13	6
					2.0	20	30	196	347	−0.20	285	−0.04	70
Mayersak et al. [8]	1	Horizontal SS	Unknown	Unknown	11.7	50	45	29	213	−0.51	168	−0.40	43
					11.7	50	45	29	213	−0.51	168	−0.40	43
Ornatskii and Vinyarskii [9]	96	Vertical Cu alloy	Contraction	Expansion	0.5	28	20	10	75	−0.81	50	−0.57	40
					0.5	28	90	70	274	−0.16	188	−0.11	224
Skinner and Loosmore [10]	98	Horizontal SS-304	$L/D = 20$	Unknown	1.2	3	5	2	28	−0.32	1	−0.24	7
					6.1	52	20	7	158	−0.06	120	0.00	33
Zeigarnik et al. [11]	20	Horizontal brass	Unknown	Unknown	4.0	62	5	5	80	−0.51	25	−0.22	9
					4.0	62	21	30	215	−0.19	93	−0.06	33
Nariai et al. [12]‡	92	Vertical SS	Unknown	Unknown	1.0	3	7	1	37	−0.16	3	−0.13	5
					3.0	50	21	1	85	−0.07	72	−0.01	70
Boyd [13]	5	Horizontal Cu–Zr alloy	$L_{uh}/D > 40$	Unknown	3.0	97	5	8	149	−0.31	24	−0.12	6
					3.0	97	41	8	149	−0.31	57	−0.05	42

Boyd [14]	5	Horizontal	$L_{uh}/D > 40$	Unknown	3.0	97	4	17	183	−0.41	51	−0.18	6
		Cu–Zr alloy			3.0	97	32	17	183	−0.41	78	−0.12	36
Inasaka and Nariai [15]	29	Vertical	Unknown	Unknown	3.0	33	4	3	63	−0.31	20	−0.18	7
		SS			3.0	33	30	10	150	−0.12	87	−0.04	45
Celata et al. [16]§	60	Vertical	L_{uh}/D not specified	L_{uh}/D	6.0	12	2.0	4	83	−0.62	54	−0.52	7
		SS-304		not specified	8.0	19	10	51	232	−0.16	193	−0.11	30
Celata et al. [17]	43	Vertical	$L_{uh}/D = 80$ (100)	L_{uh}/D	2.5	20	2.2	1	79	−0.44	19	−0.26	4
		SS-304		not specified	5.0	40	33	22	194	−0.15	113	−0.03	43
Celata et al. [18]	78	Vertical	$L_{uh}/D = 80$	L_{uh}/D	2.5	40	11	6	92	−0.46	52	−0.36	12
		SS-304		not specified	2.5	40	40	26	196	−0.19	150	−0.11	61
Celata and Mariani [19]	87	Vertical	$L_{uh}/D = 100$ (80)	L_{uh}/D	2.5	20	3	1	80	−0.46	23	−0.36	7
		SS-304		not specified	5.0	40	43	26	196	−0.15	155	−0.04	57
Gaspari and Cattadori [20]	33	Horizontal	L_{uh}/D not specified	Unknown	8.0	15	5	10	110	−0.52	83	−0.42	11
		Cu			15.0	20	15	55	186	−0.23	151	−0.18	36
Vandervort et al. [21]	202	Vertical	$L_{uh}/D \approx 10$	Unknown	0.33	1.7	8	1	40	−0.39	10	−0.28	19
		SS-304			2.7	26	42	23	183	−0.08	130	−0.02	124
Celata [22]	41	Vertical	Unknown	Unknown	0.25	40	7	1	69	−0.33	9	−0.22	10
		SS-304			1.5	40	50	9	156	−0.13	104	−0.02	68
Part I [23] of present study	174	Vertical	Contraction	Expansion	0.4	2.4	5	3	61	−1.90	32	−1.78	9
		SS-304			2.5	34	134	172	329	−0.12	305	−0.06	276
High-CHF database	1596				0.25	1.7	1.5	0.7	13	−2.47	1	−2.13	4
					15.0	97	134	196	347	−0.04	305	0.00	276

† Data obtained from Skinner and Loosmore [10]; ‡ data obtained from Inasaka [24]; § data obtained from Celata and Mariani [19].

Reference column identifies the publication by the authors who obtained the CHF data. If CHF data were not tabulated in this reference, then one of the symbols above identifies the source of the data.

Material indicates the test section material utilized in the majority of CHF tests. SS indicates stainless steel. Materials not shown include: A1 [2], type "A" Ni [10], Inconel 600, SS-316, Ni 200, and brass [21], Cu–Ni 30% [23].

Unheated entrance (exit) region refers to the section of the tube immediately upstream (downstream) of the heated length. A length-to-diameter ratio indicates an unheated section having the same diameter as the heated section. Contraction or expansion indicates an abrupt and significant change in flow diameter.

The upper and lower number in each cell of a parameter column represents the smallest and largest value, respectively, of that parameter for the acceptable subcooled CHF data in that reference. Outlet conditions were calculated using the inlet temperature from the database and an energy balance. Saturated thermophysical properties were evaluated at the pressure associated with the CHF data point (usually outlet pressure).

at the subcooled temperature. All calculations performed in the present study utilized saturated thermophysical properties based on outlet pressure since inlet pressure was rarely tabulated with the CHF data. If the outlet quality or subcooling was tabulated instead of an inlet condition, then the outlet enthalpy was determined and inlet enthalpy calculated using equation (1). Once the inlet enthalpy was determined, the inlet temperature was calculated from the equation for saturated liquid enthalpy using the secant method of iteration. Finally, each CHF data point in the database consisted of the following: tube inside diameter, heated length, mass velocity, outlet pressure, inlet temperature and measured CHF.

If both an inlet and outlet condition were tabulated by the authors of the data, then outlet quality was calculated using equation (1) and the inlet temperature from the database. This calculated outlet quality was compared to outlet quality determined from the outlet condition tabulated by the authors of the data. If these outlet qualities differed by more than 0.05 (0.10 if the pressure was greater than 75% of the critical pressure), then an energy balance was violated and the data point was discarded from further analysis. This process filtered the data for typographical errors committed by the original authors or inaccurate thermophysical properties utilized by the original authors.

3. High-CHF correlations

High-flux cooling using high mass velocity flow in small diameter tubes will become an acceptable cooling technique only when accurate design tools have been developed and thoroughly tested. Hundreds of CHF correlations have been published in the archival literature during the past fifty years. However, these correlations have not been tested with a large, error-free CHF database. The authors of this study are in the process of collecting all CHF correlations applicable to flow in uniformly heated round tubes. The present study considers only correlations applicable to subcooled high-CHF [21, 27–31] and presents a methodology for accurately evaluating the predictive ability of these correlations. Correlations not applicable to water or uniformly heated round tubes cooled by internal axial flow were not considered. Also, the original version of a correlation later revised by the authors of the correlation was rejected and only the revised correlation retained for further analysis in the present study. The earliest archival publication of a CHF correlation is cited in the list of references.

Tong [32] empirically modified a CHF model based on boundary layer separation [33] and stated that

$$Bo = CRe_D^{-0.6}, \tag{2}$$

where C was a quadratic function of x_o,

$$C = 1.76 - 7.433x_o + 12.222x_o^2. \tag{3}$$

Equation (2) is valid for large tubes ($5.1 \leqslant D \leqslant 17.8$ mm), low mass velocities ($1400 \leqslant G \leqslant 6800$ kg m^{-2} s^{-1}), and outlet qualities between -0.15 and 0.15. Although equation (2) is not applicable to high-CHF, Inasaka and Nariai [27] modified it by multiplying C by an additional term which is a function of outlet quality and pressure,

$$C = \left[1 - \frac{52.3 + 80x_o - 50x_o^2}{60.5 + (10^{-5}P)^{1.4}}\right] \times (1.76 - 7.433x_o + 12.222x_o^2), \tag{4}$$

and extended the parametric range for equation (2) ($2.0 \leqslant D \leqslant 19.1$ mm, $900 \leqslant G \leqslant 23\,100$ kg m^{-2} s^{-1}, $1 \leqslant P \leqslant 138$ bars, and $-0.35 \leqslant x_o \leqslant 0$) [34]. Celata et al. [30] also modified equation (2) by replacing C by a new function of x_o and P,

$$C = (0.216 + 4.74 \times 10^{-8}P)\Psi \tag{5}$$

where

$$\Psi = \begin{cases} 1, & x_o < -0.1 \\ 0.825 + 0.986x_o, & -0.1 < x_o < 0, \\ 1/(2 + 30x_o), & x_o > 0 \end{cases} \tag{6}$$

and by increasing the exponent of the Reynolds number to -0.5. The data utilized by Celata et al. ($0.3 \leqslant D \leqslant 25.4$ mm, $900 \leqslant G \leqslant 9000$ kg m^{-2} s^{-1}, $1 \leqslant P \leqslant 84$ bars [19]) to develop the correlation included some of the high-CHF data obtained by Ornatskii and Kichigin [3] and Ornatskii and Vinyarskii [9]. The above correlations were all based on outlet conditions, sometime referred to as local conditions since CHF is believed to occur at the outlet of a uniformly heated channel.

Bowring [35] proposed a correlation based on inlet conditions of the form

$$q_m = \frac{C_1 + C_2\Delta h_{sub,i}}{C_3 + L} = \frac{C_1/C_3 + (C_2/C_3)\Delta h_{sub,i}}{1 + L/C_3}, \tag{7}$$

where C_1 and C_2 are complicated functions of D, G, and P, and C_3 is a function of D and G. This complex correlation contains 24 adjustable constants and is valid for $2 \leqslant D \leqslant 45$ mm, $136 \leqslant G \leqslant 18\,000$ kg m^{-2} s^{-1}, and $2 \leqslant P \leqslant 190$ bars. However, it was not developed with high-CHF data since none were available to Bowring. Caira et al. [29] replaced the Bowring functions (C_1, C_2, and C_3) while maintaining the same functional form,

$$q_m = \frac{C_1 D^{C_2} G^{C_3} + C_5 D^{C_6} G^{C_7} (0.25\Delta h_{sub,i})^{C_4}}{1 + C_8 D^{C_9} G^{C_{10}} L^{C_{11}}}, \tag{8}$$

and reduced the number of adjustable constants to eleven. However, equation (8) eliminated the effect of pressure which was present in the Bowring correlation. Caira et al. [31] attempted to re-introduce the pressure effect by defining different constants in 6 pressure regions and 2 mass velocity regions, resulting in 138 adjustable constants. The correct constants had to be obtained from

Caruso [36] since the constants tabulated in Caira et al. [31] yielded CHF values many orders of magnitude above actual CHF. Both Caira et al. [29, 31] correlations were developed using the Celata and Mariani [19] CHF database.

The Vandervort et al. [21] correlation is the product of mass velocity, outlet subcooling, pressure, a diameter term and an L/D term with all variables raised to powers which are functions of diameter, mass velocity, and/or subcooling. This outlet conditions correlation contains 16 adjustable constants and was developed using the small diameter data ($0.3 \leqslant D \leqslant 3.0$ mm) in the Celata and Mariani [19] CHF database.

Shah [37] developed a CHF correlation that was originally presented in graphical form and later improved [28] and updated to an equation form suitable for computer codes. The improved correlation was based on data obtained with 23 different fluids over a broad range of parameters ($0.6 \leqslant D \leqslant 37.8$ mm, $8 \leqslant L/D \leqslant 940$, $13 \leqslant G \leqslant 24\,300$ kg m^{-2} s^{-1}, $1 \leqslant P \leqslant 207$ bars, $-1.15 \leqslant x_o \leqslant 1.0$). The correlation included criteria for choosing between an inlet or an outlet conditions based set of equations. The reader is referred to Shah [28] for additional information since the correlation as well as the calculation procedure is quite complex (26 equations and 35 adjustable constants).

The subcooled high-CHF correlations [21, 27–31] considered in the present study are quite complex having either many constants (more than ten) [21, 28, 29, 31], many equations [28], or conditional statements for choosing an equation or set of equations [28, 30, 31]. Furthermore, correlations having conditional statements allow severe discontinuities in the predicted CHF as a parameter is varied across a boundary described by one of these statements. Also, none of the correlations are entirely nondimensional except for Shah's [28]. Furthermore, the functional forms of the correlations were not based on observed trends in the CHF data, but rather the equation form was guessed and a statistical analysis performed to obtain values for the adjustable constants. The present study aims to develop a single, nondimensional equation containing as few constants as possible without using a statistical analysis but rather using trends observed in a subset of the high-CHF database.

4. Design equations—pressure drop model

CHF correlations require accurate knowledge of the pressure at burnout location (i.e., end of heated length for a uniformly heated tube) to evaluate the saturated thermophysical properties of the fluid. While mass velocity and tube diameter are easily measured, the pressure at the burnout location must often be calculated since experimental measurements are made downstream. Furthermore, most researchers provide little information, if any, regarding the nature of the outlet and inlet to the test section and, consequently, the origin of the tabulated pressure may be suspect. The present study aims to provide a comprehensive pressure drop model for flow in tubes (especially those having a total length-to-diameter ratio less than 30) with inlet and outlet plenums. The model enables the determination of the pressures at the beginning and end of the heated length which are often significantly different (especially for high mass velocity flow in small diameter tubes such as in the present study) from that measured either upstream or downstream of the test section.

The experimental results presented in Part I [23] demonstrated that the pressure drop at CHF deviated only slightly from the single-phase, adiabatic pressure drop. Thus, the flow was modeled as turbulent, single-phase liquid flow in a smooth tube. The pressure drop from the inlet plenum to the outlet plenum has contributions from the inlet contraction, wall friction within the tube (corrected for momentum flux changes), and outlet expansion,

$$\Delta P = P_{p,i} - P_{p,o} = \Delta P_c + \Delta P_f + \Delta P_e. \tag{9}$$

The pressure drops between the upstream pressure tap and inlet plenum and between the downstream pressure tap and outlet plenum were negligible compared to the pressure drop between the inlet and outlet plenums. Figure 1(a,b) illustrates the streamlines for internal flow with an abrupt contraction and expansion and defines the nomenclature utilized in the analysis. Each term in equation (9) will be treated separately in the following sections. Detailed development of the model equations is given in ref. [38].

4.1. Frictional pressure drop

The short tubes ($L_t/D = 11$) utilized in the present study have a significant fraction, if not all, of the total length corresponding to a hydrodynamic entrance region. Part of the pressure drop in the entrance region of a tube is attributable to an increase in the total fluid momentum flux, associated with the development of a velocity profile, and pressure drop calculations must take into consideration any variation in momentum flux as well as the effects of surface shear forces. The combined effects of surface shear and momentum flux have been incorporated in a single mean apparent friction factor f_{app}. The pressure drop across the tube can then be evaluated from

$$\Delta P_f = P_1 - P_2 = \frac{G^2}{2\rho_f}\left(4 f_{app}\frac{L_t}{D}\right). \tag{10}$$

Deissler [39] solved the momentum integral equation for developing flow without heat transfer in a smooth, circular tube with constant properties and a turbulent boundary layer having a uniform velocity profile orig-

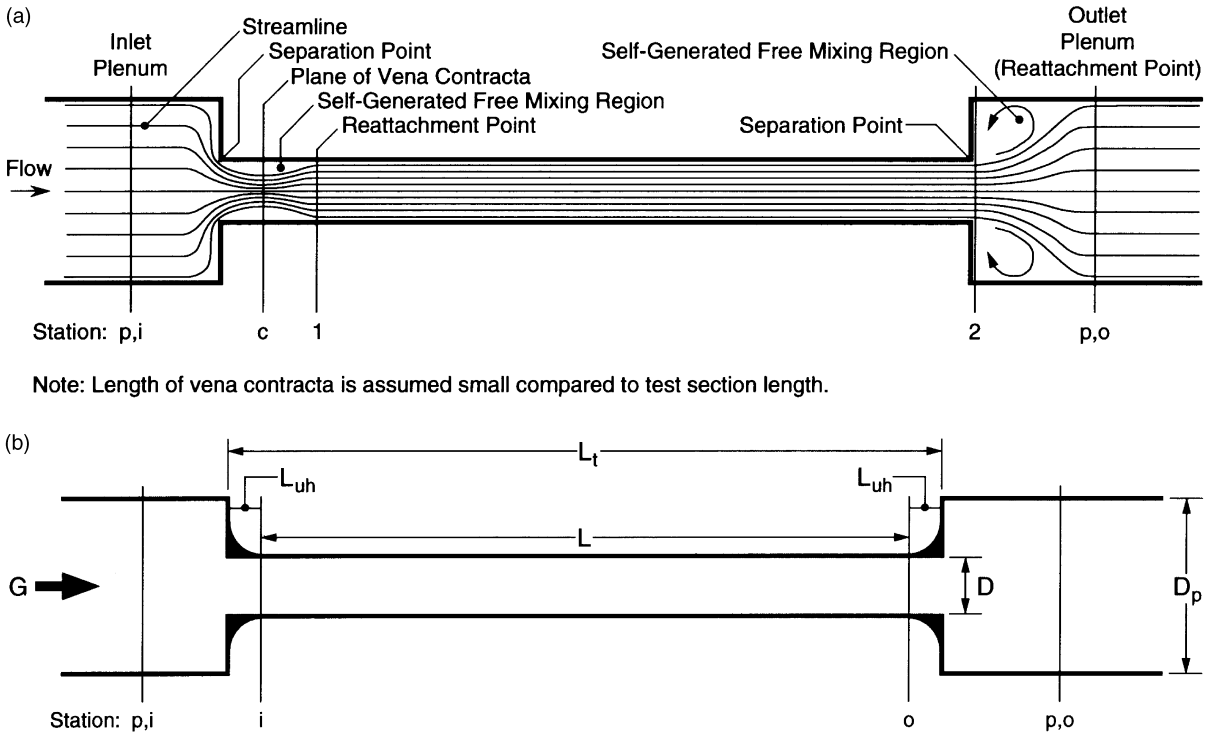

Fig. 1. Flow model of an abrupt contraction and expansion at the test section inlet and outlet, respectively, showing (a) streamlines and (b) test section geometry.

inating at the entrance. The mean apparent friction factor in the turbulent entry region was graphically presented as a function of the total length-to-diameter ratio ($0.25 < L_t/D < 20$) for several Reynolds numbers ($1\times10^4 \leqslant Re_D \leqslant 1\times10^5$). The data symbols shown in Fig. 2 correspond to locations on the theoretical curves in Deissler. This data was curve-fitted by the present authors to obtain an expression for f_{app},

$$f_{app} = \left(0.2295 + 0.6074\frac{D}{L_t}\right) Re_D^{(-0.3305-0.02154D/L_t)}. \quad (11)$$

Equation (11) replaces the equation from Phillips et al. [40] which was developed from, but did not correctly reproduce, the data from Deissler. Note that single-phase Reynolds numbers for the data in Part I [23] of the present study were from 4.4×10^3 to 1.2×10^5, barely exceeding the applicable range of equation (11).

4.2. Contraction pressure drop

Turbulent flow through an abrupt contraction separates at the entrance to the smaller flow area and forms turbulent eddies about the resultant jet. The jet accelerates and contracts until a minimum area is attained at the vena contracta. The jet then decelerates and expands to fill the smaller diameter tube as pipe flow is re-established. The change in static pressure across an abrupt contraction is the sum of a reversible (ideal) change associated solely with the change in velocity due to the change in flow area (first term) and an irreversible loss due to viscous friction and formation of eddies at the front of the contraction and at the vena contracta (second term) [41],

$$\Delta P_c = P_{p,i} - P_1 = \frac{G^2}{2\rho_f}[(1-\beta_c^2) + K_c]. \quad (12)$$

where β_c is the ratio of tube flow area to inlet plenum flow area and the contraction loss coefficient is given by

$$K_c = \frac{1 - E_{p,i}\beta_c^2 C_c^2 - 2C_c + 2C_c^2 M_1}{C_c^2} - (1-\beta_c^2). \quad (13)$$

The jet contraction ratio, C_c, which is the ratio of the cross-sectional flow area of the jet at the vena contracta to the area of the surrounding tube, was measured by Weisbach [42] for water flow in short pipes. Although, this ratio is somewhat dependent on the Reynolds number in turbulent flow, the generally accepted practice is to curve-fit the flow independent data of Weisbach as a function of the area ratio β_c [43],

$$C_c = \frac{A_c}{A} = 0.61375 + 0.13318\beta_c - 0.26095\beta_c^2 + 0.51146\beta_c^3. \quad (14)$$

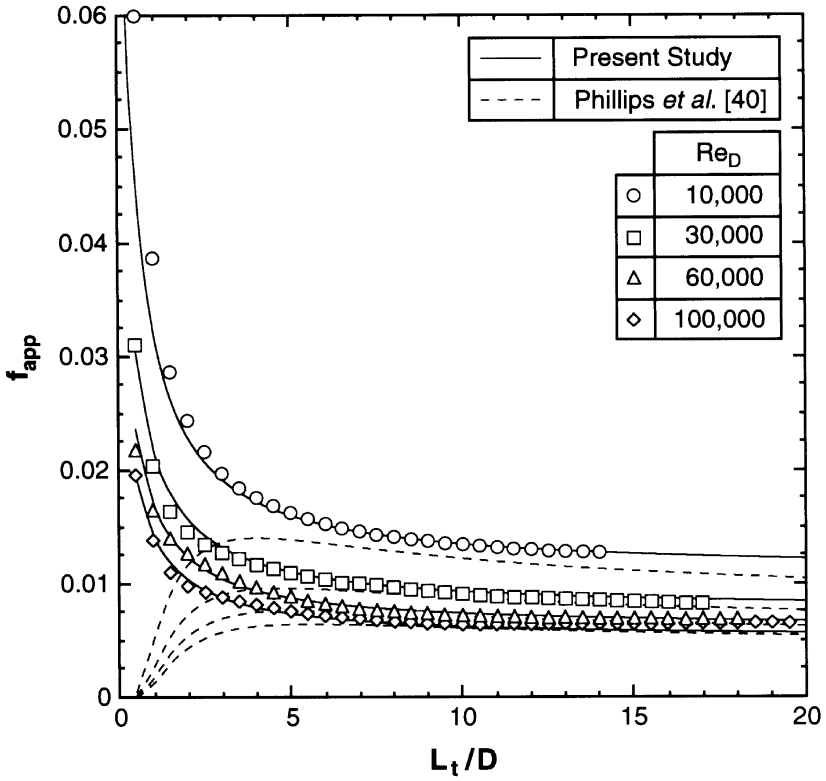

Fig. 2. Variation of apparent mean friction factor with total length-to-diameter ratio for the turbulent entry region of a smooth tube. Data from theoretical analysis in Deissler [39].

The kinetic energy and momentum correction factors account for the variation of velocity at a given section,

$$E_{p,i} = \frac{1}{A_{p,i}} \int_{A_{p,i}} \left(\frac{u}{U_{p,i}} \right)^3 dA \tag{15}$$

and

$$M_1 = \frac{1}{A} \int_A \left(\frac{u}{U_1} \right)^2 dA \tag{16}$$

where $U_{p,i}$ is the mean velocity in the inlet plenum and U_1 is the mean velocity at section 1. The entrance losses described by equation (13) include both pressure losses due to the expansion of the fluid following the vena contracta and changes in pressure due to the change in momentum as the velocity profile is established in the small diameter tube. Thus, the estimate of the total pressure drop will be a conservative upper limit since the pressure change associated with the change in velocity profile is accounted for in both the mean apparent friction factor and entrance loss coefficient.

The flow in inlet plenum is assumed to be fully developed turbulent flow (i.e., uniform velocity profile) so that the kinetic energy correction factor is one. Kays [41] derived a semi-empirical expression for the momentum correction factor for turbulent flow from the Kármán–Prandtl relations,

$$M_1 = 1 + 0.05884\sqrt{4f} + 1.09068(4f), \tag{17}$$

where f in this equation is the Fanning friction factor for fully developed turbulent flow in a smooth pipe,

$$f = 0.049 Re_D^{-0.2}, \tag{18}$$

which approximates the Prandtl–Kármán–Nikuradse relation in the range $3 \times 10^4 < Re_D < 1 \times 10^6$ [44]. Note that, in the development of equation (17), Kays increased the coefficient in equation (18) from the conventional value of 0.046 for smooth surfaces to 0.049 to better describe heat exchangers which were the focus of his study.

4.3. Expansion pressure recovery

The static pressure in an abrupt expansion rises as the result of the exchange of kinetic energy of the high velocity flow for the potential energy of pressure in the lower velocity flow. The change in static pressure across an abrupt expansion is the sum of a reversible (ideal) pressure rise associated solely with the increase in flow

area (second term) and an irreversible loss associated with viscous friction and free expansion (first term),

$$\Delta P_e = P_2 - P_{p,o} = \frac{G^2}{2\rho_f}[K_e - (1-\beta_e^2)], \quad (19)$$

where β_e is the ratio of tube flow area to outlet plenum flow area and the expansion loss coefficient is given by

$$K_e = 1 - 2M_2\beta_e + \beta_e^2(2M_{p,o} - 1). \quad (20)$$

The momentum correction factors, M_2 and $M_{p,o}$, account for the variation of axial velocity at section 2 and in the outlet plenum. The flow at these locations is assumed to be fully developed turbulent flow (i.e., fairly uniform velocity profile) so that both correction factors become equal to unity.

4.4. Outlet pressure

The outlet pressure at the end of the heated length, P_o, is determined from the measured pressure in the outlet plenum,

$$P_o = P_{p,o} + \Delta P_e + \Delta P_{f,uh}, \quad (21)$$

where the expansion pressure drop is given by equation (19) and the frictional pressure drop across the unheated region of the tube at the outlet is given by

$$\Delta P_{f,uh} = P_o - P_2 = \frac{G^2}{2\rho_f}\left(4f_{app}\frac{L_{uh}}{D}\right), \quad (22)$$

where, for simplicity, the mean apparent friction factor is the same as that used to compute the frictional pressure drop across the entire tube. In the present study, the unheated length of the tube at the outlet is assumed equal to that at the inlet and given by

$$L_{uh} = 0.5(L_t - L), \quad (23)$$

where both the total length, L_t, and heated length, L, were measured using a microscope and a micrometer. The inlet pressure at the beginning of the heated length is determined in a similar manner.

4.5. Comparison of pressure drop model with experimental data

The pressure drop model for turbulent, single-phase liquid flow in a short, smooth tube with inlet and outlet plenums is summarized in Table 3. The predicted pressure drop and inlet and outlet pressure at CHF are tabulated in Table 1 of Part I [23]. A comparison of the predicted pressure drop with pressure drop measured at the onset of CHF is shown in Fig. 3(a). The wide range of tube diameters and mass velocities resulted in a broad range of pressure drops from 0.2 to 153 bars. The usefulness of this single-phase model as a predictive tool for high-high-flux, subcooled flow boiling is illustrated by this plot with most data falling within a $\pm 40\%$ error band. Only a single data point deviated more than 40% for pressure drops above 5 bars corresponding to the high-CHF data obtained at high mass velocities ($G \geqslant 20\,000$ kg m^{-2} s^{-1}). Below 5 bars, 14 of 15 data points which deviated more than 40% were underpredicted by the model.

Figure 3(b) illustrates the relative contributions to the contraction, frictional and expansion pressure drops to the total pressure drop from inlet to outlet plenum. The cases shown in Fig. 3(b), which are representative of the present study, indicate that the contraction pressure drop is usually the largest fraction of the entire pressure drop and the expansion pressure recovery is always the smallest. The contribution of the contraction pressure drop increases significantly with increasing tube diameter causing a decrease in the contribution of the frictional pressure drop and an increase in the contribution of the expansion pressure recovery. Thus, any abnormalities present in the inlet region would have a significant effect on the model predictions for the larger diameter tubes. The model assumes a square-edged entrance to the heated tube. A slightly-rounded entrance (i.e., gradual contraction) or protrusion of the tube into the inlet plenum (i.e., re-entrant) would cause the contraction pressure drop to decrease or increase, respectively, from the model prediction. Therefore, considerable care was taken during test section fabrication to eliminate these possibilities.

The results obtained from the pressure drop model clearly illustrate the importance of presenting detailed pressure measurements with CHF data and also a description of the flow path upstream and downstream of the heated section. Ornatskii and Vinyarskii [9] obtained ultra-high-CHF data under conditions very similar to those of the present study (high mass velocity flow in small diameter tubes with an abrupt inlet contraction and abrupt outlet expansion). However, their data were not tabulated with a specific pressure value, but rather a range of pressures over which a set of data was acquired. The location of the pressure measurement was also not given. Consequently, the authors of the present study were unwilling to utilize the data from Ornatskii and Vinyarskii in the development of a new correlation because of imprecise thermophysical properties resulting from inept reporting of pressure.

The present study (including Part I [23]) is the only high-CHF study in the literature which provided detailed pressure measurements and a model from which to accurately predict the pressure at the end of the heated length (CHF location for subcooled flow boiling) and the corresponding local thermophysical properties of the saturated fluid. The pressure drop model was validated with short tubes (total length-to-diameter ratio less than 30) having upstream and downstream flow areas significantly larger than the flow area in the test section. Nevertheless, the model is equally valid for subcooled flow boiling in longer tubes or in the absence of an inlet contraction or outlet expansion. The pressure drop model was not applied to CHF data from previous studies; lack of infor-

Table 3
Pressure drop model for turbulent, single-phase liquid flow in a short, smooth tube with inlet and outlet plenums

Total pressure drop	$\Delta P = P_{p,i} - P_{p,o} = \Delta P_c + \Delta P_f + \Delta P_e$
Contraction pressure drop	$\Delta P_c = P_{p,i} - P_1 = \frac{G^2}{2\rho_f}[(1-\beta_c^2) + K_c]$
	$K_c = \frac{1 - E_{p,i}\beta_c^2 C_c^2 - 2C_c + 2C_c^2 M_1}{C_c^2} - (1-\beta_c^2)$
	$\beta_c = \frac{A}{A_{p,i}} = \left(\frac{D}{D_p}\right)^2$
	$C_c = \frac{A_c}{A} = 0.61375 + 0.13318\beta_c - 0.26095\beta_c^2 + 0.51146\beta_c^3$ [43]
	$E_{p,i} = \frac{1}{A_{p,i}}\int_{A_{p,i}} \left(\frac{u}{U_{p,i}}\right)^3 dA \approx 1$
	$M_1 = \frac{1}{A}\int_A \left(\frac{u}{U_1}\right)^2 dA = 1 + 0.05884\sqrt{4f} + 1.09068(4f), \quad f = 0.049 Re_D^{-0.2}$ [41]
Frictional pressure drop	$\Delta P_f = P_1 - P_2 = \frac{G^2}{2\rho_f}\left(4 f_{app}\frac{L_t}{D}\right)$
	$f_{app} = \left(0.2295 + 0.6074\frac{D}{L_t}\right) Re_D^{(-0.3305 - 0.02154 D/L_t)}$
Expansion pressure drop	$\Delta P_e = P_2 - P_{p,o} = \frac{G^2}{2\rho_f}[K_e - (1-\beta_e^2)]$
	$K_e = 1 - 2M_2\beta_e + \beta_e^2(2M_{p,o} - 1)$
	$\beta_e = \frac{A}{A_{p,o}} = \left(\frac{D}{D_p}\right)^2$
	$M_2 = \frac{1}{A}\int_A \left(\frac{u}{U_2}\right)^2 dA \approx 1$
	$M_{p,o} = \frac{1}{A_{p,o}}\int_{A_{p,o}} \left(\frac{u}{U_{p,o}}\right)^2 dA \approx 1$
Inlet and outlet pressure	$P_i = P_{p,o} + \Delta P_e + \Delta P_f - \Delta P_{f,uh}$
	$P_o = P_{p,o} + \Delta P_e + \Delta P_{f,uh}$
	$\Delta P_{f,uh} = \frac{G^2}{2\rho_f}\left(4 f_{app}\frac{L_{uh}}{D}\right)$

Liquid density and liquid dynamic viscosity are evaluated at the inlet temperature.
Range of applicability for M_1 is $2000 \leqslant Re_D \leqslant 20\,000$ [41] and for f_{app} is $10\,000 \leqslant Re_D \leqslant 100\,000$ [39].

mation forced the authors of the present study to assume that the pressure tabulated with the CHF data in Refs. [1–22] corresponded to the end of the heated length.

5. Design equations—subcooled CHF correlation

CHF correlations are classified as either an inlet (upstream) conditions correlation based on independent variables such as inlet enthalpy and heated length,

$$q_m = \mathrm{fn}(D, L, G, P, h_i), \tag{24}$$

or an outlet (local) conditions correlation based on a dependent variable such as outlet enthalpy,

$$q_m = \mathrm{fn}(D, G, P, h_o). \tag{25}$$

In nondimensional form, equations (24) and (25) become

$$Bo = \mathrm{fn}\left(\frac{L}{D}, We_D, \frac{\rho_f}{\rho_g}, x_i\right) \tag{26}$$

and

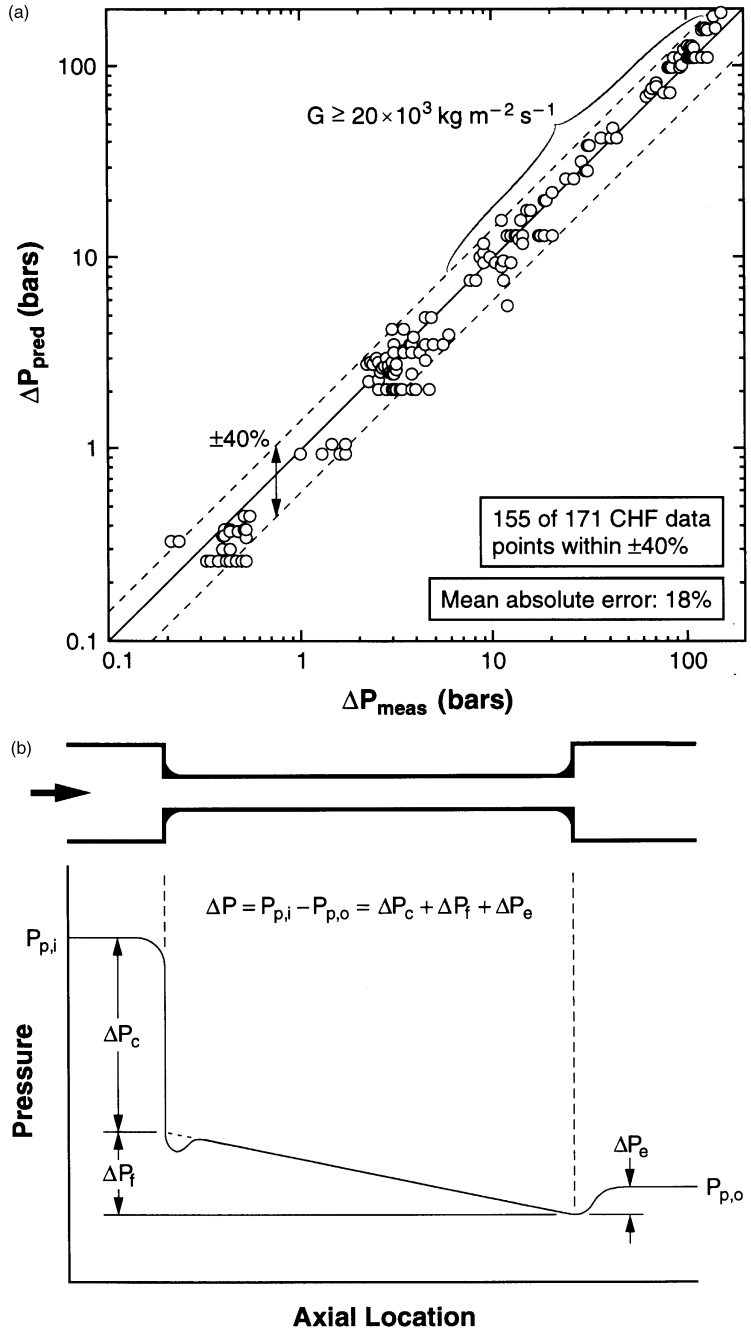

Measured					Predicted			
D (mm)	L_t (mm)	$P_{p,o}$ (bars)	$G\times10^{-3}$ (kg m^{-2} s^{-1})	ΔP (bars)	ΔP (bars)	$\frac{\Delta P_c}{\Delta P}$	$\frac{\Delta P_f}{\Delta P}$	$\frac{\Delta P_e}{\Delta P}$
0.406	11.0	31.0	40.0	19.3	19.9	0.59	0.43	-0.02
			100.0	102.4	109.9	0.66	0.35	-0.02
0.902	11.0	31.0	40.0	13.1	13.1	0.87	0.25	-0.11
			100.0	67.6	76.2	0.93	0.19	-0.12

Fig. 3. (a) Comparison of predicted pressure drop, assuming single-phase flow, with measured pressure drop at CHF. (b) Contribution of predicted contraction, frictional, and expansion pressure drop to total pressure drop.

$$Bo = \mathrm{fn}\left(We_D, \frac{\rho_f}{\rho_g}, x_o\right), \tag{27}$$

respectively. The ratio of saturated liquid density to saturated vapor density was chosen as the dimensionless group to represent mostly the effect of pressure.

An outlet conditions correlation such as equation (25) or (27) can be transformed into an inlet conditions correlation such as equation (24) or (26) by using the energy balance given by equation (1). In nondimensional form, the energy balance equation becomes

$$x_o = x_i\left(\frac{h_{fg,i}}{h_{fg,o}}\right) + \frac{h_{f,i} - h_{f,o}}{h_{fg,o}} + 4\frac{L}{D}\frac{q_m}{Gh_{fg,o}}, \tag{28}$$

where x_i and x_o are the thermodynamic equilibrium qualities with saturated thermophysical properties evaluated at the inlet and outlet pressure, respectively. The subscripts i and o in equation (28) indicate the pressure at which to evaluate the enthalpy of saturated liquid and latent heat of vaporization. Equation (28) can also be written as

$$x_o = x_{i,*} + 4Bo\frac{L}{D}, \tag{29}$$

where all saturated thermophysical properties are evaluated at the outlet pressure, including those appearing in the pseudo-inlet quality, $x_{i,*}$. If the pressure drop across the heated length is relatively small, then the inlet and outlet pressures are approximately equal as are the pseudo- and true-inlet qualities.

The authors of the present study elected to develop nondimensional correlations in the form of equations (26) and (27) because of their simplicity. An inlet conditions and an outlet conditions correlation were developed concurrently to illustrate the differing viewpoints. The parametric study in Part I [23] revealed the following relationships between the independent variables and CHF:

1. For constant L, P, and x_i, CHF is proportional to a negative power of D which is independent of G (see Fig. 10 in Part I).
2. For constant D and T_i, CHF is proportional to a negative power of L/D which is independent of G, P, and x_i (see Fig. 11 in Part I).
3. For constant L and T_i, CHF is proportional to a positive power of G which is independent of P and x_i (see Fig. 12 in Part I).
4. For constant D, L/D, and P, CHF decreases linearly with increasing x_i (see Fig. 13(b) in Part I). Thus, for a relatively low pressure drop, CHF must also vary linearly with x_o since x_i and x_o are linearly related by an energy balance (equation (29)).
5. Effect of pressure on CHF was not determined since data were not obtained with inlet (or outlet) quality held constant while pressure was varied (see Fig. 14 in Part I).

The above trends immediately lead one to conclude that possible correlations are

$$Bo = We_D^{c_1}\left(\frac{L}{D}\right)^{c_2}(f_1 - f_2 x_i) \tag{30}$$

and

$$Bo = We_D^{c_1}(f_3 - f_4 x_o), \tag{31}$$

where the functions of f_1, f_2, f_3, and f_4 may be constants or functions of density ratio.

The constants and functions in equations (30) and (31) must be determined using several sets of CHF data in which all but one of the dimensionless terms appearing on the right-hand side of equations (26) and (27) are held constant. The data from Part I [23] of the present study, Ornatskii and Kichigin [3, 5], and Ornatskii [7] were the only data available in the literature which were systematically obtained over a broad range of pressure. While the data from Part I were obtained over a broad range of mass velocity for a given pressure and inlet and outlet quality, the data from Ornatskii and Kichigin [3, 5] and Ornatskii [7] were obtained over a broad range of inlet and outlet quality for a given pressure and mass velocity. Thus, the combination of these data proved very effective in the systematic development of new, superior CHF correlations based solely on observed parametric trends.

5.1. Effect of mass velocity on CHF

The constant c_1 was determined using 48 data points from Part I [23] obtained with constant diameter, length, and inlet temperature ($D = 0.902$ mm, $L_t = 11$, $5.1 < L/D < 6.8$, $T_i = 25^\circ$C). Figure 4 shows the effect of Weber number on boiling number for eight pressures from 3.4 to 172 bars. Mass velocities ranged from 5000 to 40 000 kg m^{-2} s^{-1}. The few data points above 40 000 kg m^{-2} s^{-1} were excluded because they were obtained at only two pressures, 31.0 and 100 bars. The data were curve-fitted with an equation of the form

$$Bo \propto We_D^{c_1}, \tag{32}$$

where the constant of proportionality, but not c_1, was allowed to change with pressure. c_1 was found to be -0.235 indicating that CHF is approximately proportional to the square root of mass velocity at all pressures, supporting the result obtained in Part I [23]. For a given set of data taken at the same pressure, inlet quality was constant and outlet quality varied by less than 10% (essentially, only mass velocity and CHF changed). Hence, these results apply to both equations (30) and (31).

5.2. Effect of pressure and quality on CHF

In Part I [23], limited control over inlet temperature prevented the acquisition of sufficient data at different

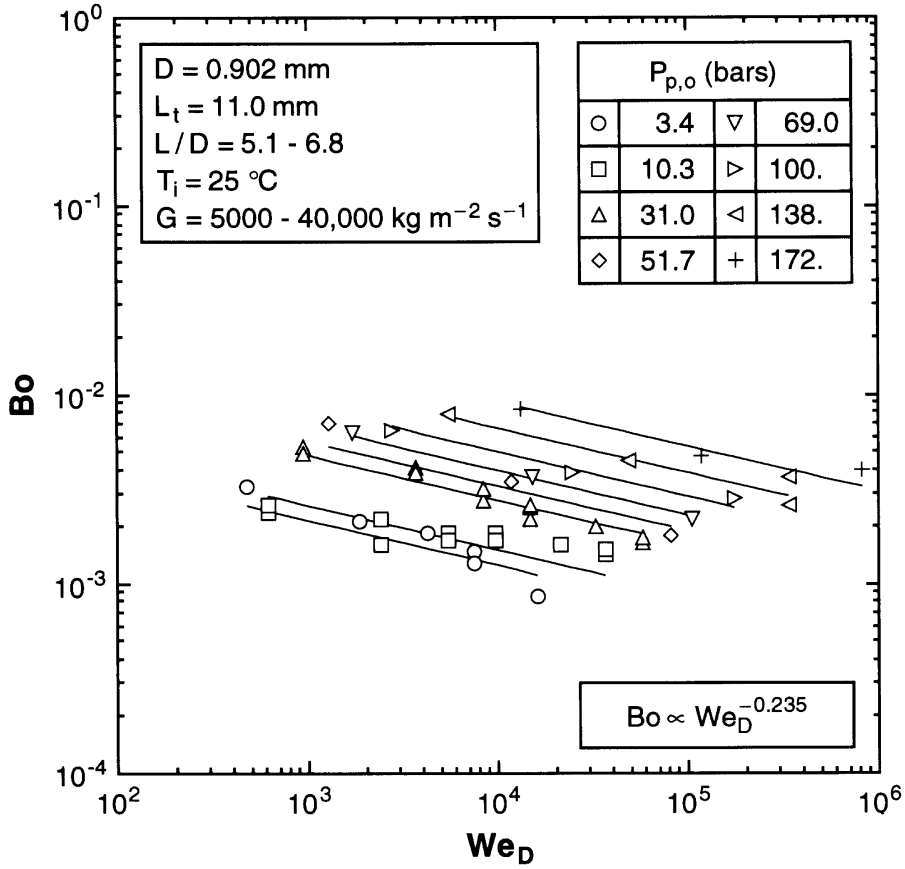

Fig. 4. Effect of Weber number on boiling number for CHF data from Part I [23] of the present study.

pressures with a broad range of inlet qualities. Thus, the dependence of CHF on inlet and outlet quality was investigated using 399 data points from Ornatskii and Kichigin [3, 5] and Ornatskii [7]. These data were obtained with $D = 2$ mm, $L/D = 20$, $5000 \leqslant G \leqslant 30\,000$ kg m^{-2} s^{-1}, and $9.8 \leqslant P \leqslant 196$ bars. Data from two different institutions were also required since Ornatskii and Kichigan [3, 5] and Ornatskii [7] did not obtain a set of data with constant inlet temperature, thus, prohibiting the application of the procedure for determining c_1 from their data. Note that, unlike Ornatskii and Vinyarskii [9], Ornatskii and Kichigan [3, 5] and Ornatskii [7] provided tabulated values of the outlet pressure. At each of nine different pressures, the data were curve-fitted with equations of the form

$$\frac{Bo}{We_D^{c_1}} = f_1 - f_2 x_i \tag{33}$$

and

$$\frac{Bo}{We_D^{c_1}} = f_3 - f_4 x_o, \tag{34}$$

where the exponent of the Weber number was already determined as discussed in the preceding section and the L/D term in equation (30) is constant ($L/D = 20$ for all data from refs [3, 5, 7]). Figure 5(a) and (b) show data and curve-fits at pressures of 25 and 147 bars for equations (33) and (34), respectively. The data and curve-fits exhibit similar agreement at the other seven pressures which are not shown. Figure 6(a) and (b) show the effect of density ratio and, hence, pressure on the functions f_1, f_2, f_3, and f_4. Except for the data points at 9.8 bars, the data were linear in logarithmic coordinates. At relatively low pressures, the combination of the lowest possible quality being relatively high (difference between local fluid enthalpy and saturated liquid enthalpy is relatively small even when highly subcooled) and f_1 and f_3 being so small yields $-f_2 x_i >> f_1$ and $-f_4 x_o >> f_3$. Thus, the values of f_1 and f_3 determined using the procedure illustrated in Fig. 6(a) and (b) become inconsequential at low pressure. The remaining data at pressures above 9.8 bars were curve-fit with an equation of the form

$$f_i = a_i (e_f/e_g)^{b_i}, \tag{35}$$

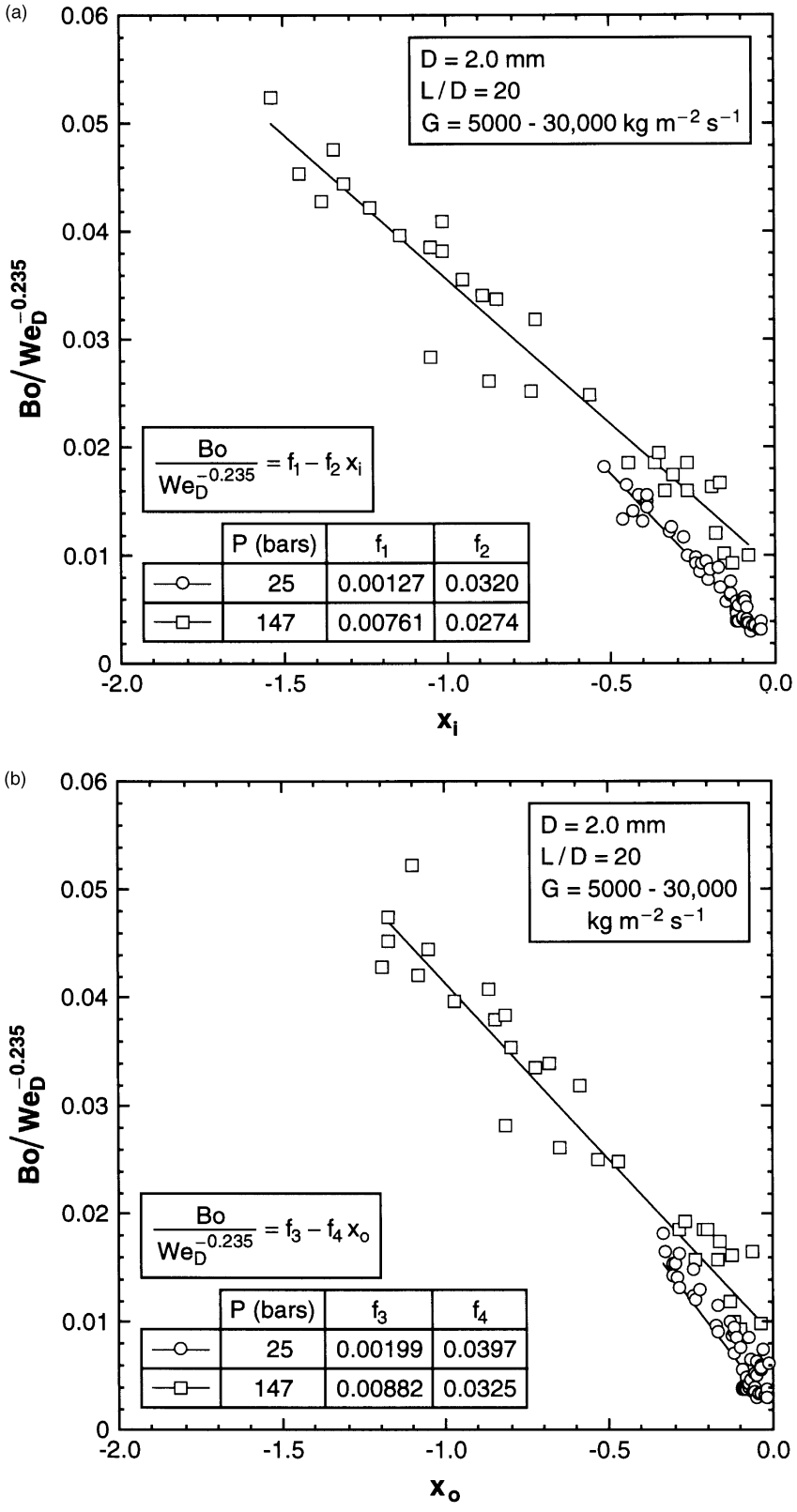

Fig. 5. Effect of (a) inlet and (b) outlet quality on boiling number for CHF data from Ornatskii and Kichigin [3, 5].

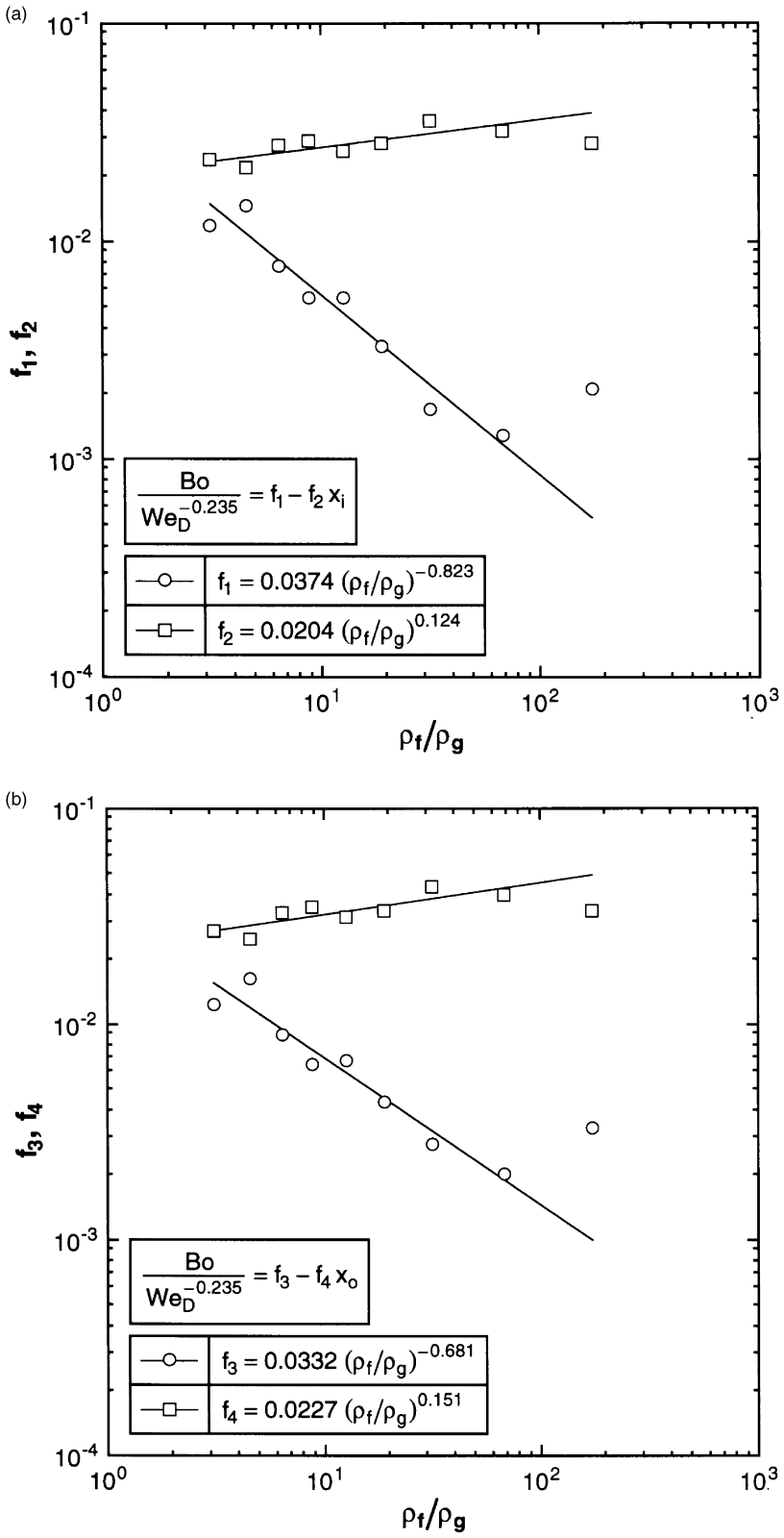

Fig. 6. Effect of density ratio on the relationship between quality and dimensionless CHF for correlation based on (a) inlet or (b) outlet quality.

where $i = 1, 2, 3$, or 4. Equations (33) and (34) have now become

$$\frac{Bo}{We_D^{c_1}} = a_1 \left(\frac{\rho_f}{\rho_g}\right)^{b_1} - a_2 \left(\frac{\rho_f}{\rho_g}\right)^{b_2} x_i \tag{36}$$

and

$$\frac{Bo}{We_D^{c_1}} = a_3 \left(\frac{\rho_f}{\rho_g}\right)^{b_3} - a_4 \left(\frac{\rho_f}{\rho_g}\right)^{b_4} x_o, \tag{37}$$

where all constants are known and given in Fig. 6(a) and (b). Rearranging equations (36) and (37) yields

$$Bo = a_1 We_D^{c_1} \left(\frac{\rho_f}{\rho_g}\right)^{b_1} \left[1 - \frac{a_2}{a_1}\left(\frac{\rho_f}{\rho_g}\right)^{b_2-b_1} x_i\right] \tag{38}$$

and

$$Bo = a_3 We_D^{c_1} \left(\frac{\rho_f}{\rho_g}\right)^{b_3} \left[1 - \frac{a_4}{a_3}\left(\frac{\rho_f}{\rho_g}\right)^{b_4-b_3} x_o\right]. \tag{39}$$

where the terms in brackets represent the effect of liquid subcooling on CHF. While the outlet conditions correlation, equation (39), is now complete, the effect of heated length-to-diameter ratio has yet to be accounted for in the inlet conditions correlation, equation (38).

5.3. Effect of heated length-to-diameter ratio on CHF

The effect of heated length-to-diameter ratio, L/D, was isolated using data from Part I [23] since the data from Ornatskii and Kichigan [3, 5] and Ornatskii [7] were obtained only with $L/D = 20$. CHF data from Part I, obtained by varying the tube length at a single pressure and two mass velocities, were curve-fitted as shown in Fig. 7 with an equation of the form

$$\frac{Bo}{We_D^{c_1}\left(\frac{\rho_f}{\rho_g}\right)^{b_1}\left[1 - a_{2'}\left(\frac{\rho_f}{\rho_g}\right)^{b_2-b_1} x_{i,*}\right]} = a_{1'}\left(\frac{L}{D}\right)^{c_2}, \tag{40}$$

where $a_{2'} = a_2/a_1$ and $a_{1'}$ is a new constant of proportionality. c_2 was determined to be -0.321, which is consistent with the results from Part I [23]. Since c_2 is negative, equation (40) shows that CHF decreases as L/D increases until outlet quality calculated from inlet quality and predicted CHF becomes positive, at which point, the correlation is no longer valid. This inlet conditions correlation has six adjustable constants, one more than the outlet conditions correlation, equation (39).

The CHF data utilized to develop equation (40) had a pressure drop across the heated length (predicted with the pressure drop model developed in the present study) that was less than 5% of the inlet pressure. Accordingly, the difference between the true-inlet quality (based on inlet pressure) and pseudo-inlet quality (based on outlet pressure) was small. Thus, the pressure at which to evaluate saturated thermophysical properties was inconsequential to the development of this correlation. Preliminary testing of the correlation with data having relatively larger pressure drops revealed that the correlation was somewhat more accurate when saturated properties were evaluated at the outlet pressure. Also, the outlet pressure was predicted with higher accuracy than the inlet pressure because the expansion pressure recovery was always a small fraction of the total pressure drop compared with that of the contraction pressure drop (see Fig. 3(b)). Furthermore, only the outlet pressure was reported in a large majority of the data in the high-CHF database. The present authors recommend evaluating saturated thermophysical properties at the outlet pressure corresponding to the end of the heated length; thus, the pseudo-inlet quality replaced the true-inlet quality in equation (40).

5.4. Transformation of the outlet conditions correlation

As discussed earlier, an energy balance can transform an outlet (local) conditions correlation based on a dependent variable (e.g., h_o or x_o) into an inlet conditions correlation based on independent variables (e.g., L or L/D and h_i or x_i). Substitution of equation (29) into the outlet conditions correlation, equation (39), yields an inlet conditions correlation,

$$Bo = \frac{a_3 We_D^{c_1}\left(\frac{\rho_f}{\rho_g}\right)^{b_3}\left[1 - \frac{a_4}{a_3}\left(\frac{\rho_f}{\rho_g}\right)^{b_4-b_3} x_{i,*}\right]}{1 + 4a_4 We_D^{c_1}\left(\frac{\rho_f}{\rho_g}\right)^{b_4}\left(\frac{L}{D}\right)}, \tag{41}$$

where all saturated thermophysical properties are evaluated at the outlet pressure. Note that this correlation does not require knowledge of the inlet pressure. Both inlet conditions correlations exhibit the effect of L/D on CHF but in different manners; equation (41) has one fewer constant since an energy balance was utilized to infer the effect of L/D on CHF. The outlet conditions correlation does not show the effect of L/D since this correlation hypothesizes that CHF is only a function of local conditions at CHF and unaffected by heated length (see equation (25)).

5.5. Summary

The final correlations developed in this study include the two inlet conditions correlations and one outlet conditions correlation shown in Table 4. The inlet conditions correlations are based on independent variables (L/D, x_i) and the outlet conditions correlation is based on a local, dependent variable (x_o). The form of one inlet conditions correlation, equation (40), and the outlet conditions correlation, equation (39), were inferred from the experimental CHF trends observed in Part I [23] of the present study. The other inlet conditions correlation, equation

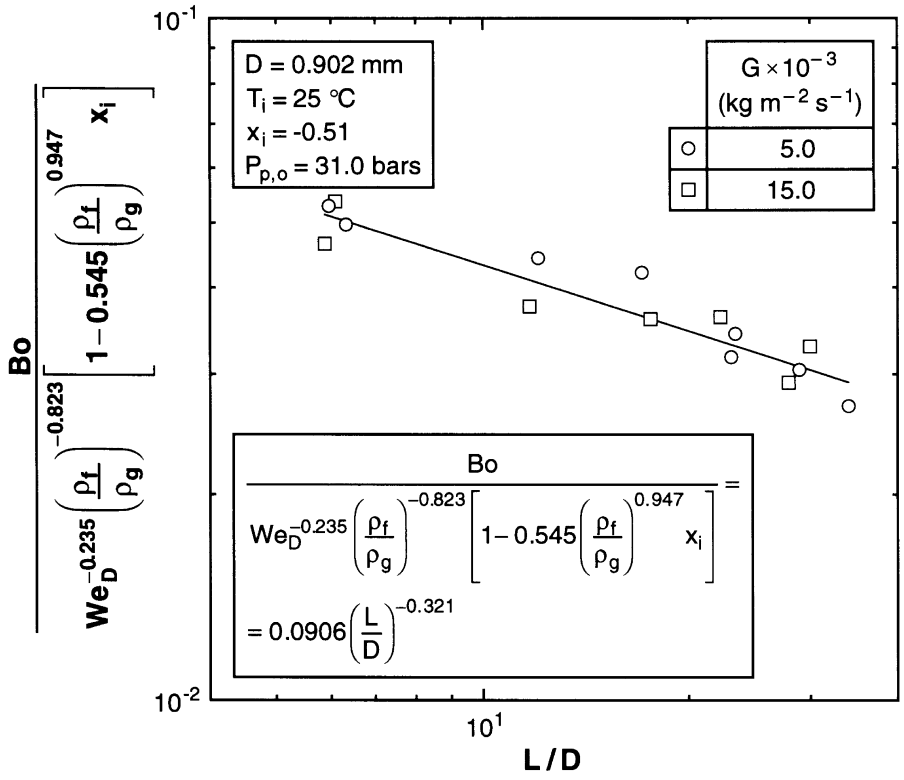

Fig. 7. Effect of heated length-to-diameter ratio on inlet conditions correlation for CHF data from Part I [23] of the present study.

Table 4
Subcooled high-CHF correlations developed in the present study

Correlation			Constants	
Inlet	$Bo = a_{1'} We_D^{c_1} \left(\frac{L}{D}\right)^{c_2} \left(\frac{\rho_f}{\rho_g}\right)^{b_1} \left[1 - a_{2'} \left(\frac{\rho_f}{\rho_g}\right)^{b_2 - b_1} x_{i,*}\right]$	(40)	$a_{1'} = 0.0906$	$b_2 = 0.124$
			$a_{2'} = 0.545$	$c_1 = -0.235$
			$b_1 = -0.823$	$c_2 = -0.321$
Outlet	$Bo = a_3 We_D^{c_1} \left(\frac{\rho_f}{\rho_g}\right)^{b_3} \left[1 - \frac{a_4}{a_3} \left(\frac{\rho_f}{\rho_g}\right)^{b_4 - b_3} x_o\right]$	(39)		
			$a_3 = 0.0332$	$b_4 = 0.151$
Inlet (recommended)	$Bo = \frac{a_3 We_D^{c_1} \left(\frac{\rho_f}{\rho_g}\right)^{b_3} \left[1 - \frac{a_4}{a_3} \left(\frac{\rho_f}{\rho_g}\right)^{b_4 - b_3} x_{i,*}\right]}{1 + 4 a_4 We_D^{c_1} \left(\frac{\rho_f}{\rho_g}\right)^{b_4} \left(\frac{L}{D}\right)}$	(41)	$a_4 = 0.0227$	$c_1 = -0.235$
			$b_3 = -0.681$	

Parametric range of the correlations corresponds to the parametric range of the acceptable subcooled CHF data in Table 2.
Saturated thermophysical properties are evaluated at the outlet pressure corresponding to the end of the heated length.
The inlet conditions correlation (equation (41)) is recommended for predicting subcooled CHF with water flow in a uniformly heated tube.

(41), was obtained from the outlet conditions correlation using an energy balance and, thus, these two correlations have the same five constants. The unknown constants were systematically determined from the parametric

trends in a subset [3, 5, 7, 23] of the high-CHF database and not nonlinear regression with the entire database. The saturated thermophysical properties appearing in the correlations are evaluated at the outlet pressure corresponding to the end of the heated length.

6. Statistical assessment of CHF correlations

6.1. *Methodology*

The present study utilized the following methodology in assessing the predictive capabilities of the CHF correlations:

1. Thermophysical properties were evaluated at the temperature specified by the correlation using equations developed by the authors of the present study from published data [45, 46]. The correlations considered in the present study all specified the saturation temperature corresponding to the outlet pressure.
2. Evaluating an inlet conditions correlation [28, 29, 31] was rather straight forward since all variables appearing in the correlation were known a priori except for CHF. Outlet conditions correlations [21, 27, 28, 30] were evaluated by calculating the required outlet variable from the experimental data and substituting this value into the correlation. The debate over using this direct substitution method rather than an energy (heat) balance method has been discussed by the present authors in a prior publication [47] as well as by many others [48–55] and will not be repeated here. Siman-Tov [56] provided an especially noteworthy discussion on this issue which was in complete agreement with the opinions of the present authors.
3. Negative qualities were always evaluated using enthalpy subcooling instead of the product of liquid specific heat and temperature subcooling.
4. Since the outlet was subcooled for almost all data in the high-CHF database, bulk liquid temperature at the outlet was evaluated from the outlet enthalpy determined using equation (1). This was necessary for determining the outlet subcooling, $\Delta T_{\mathrm{sub,o}}$, required in the Vandervort et al. [21] correlation.
5. An underpredicted CHF does not violate any conditions, but, occasionally, an outlet conditions correlation may overpredict CHF and yield an inlet temperature below the triple-point temperature (0.01°C for water) when the inlet temperature is calculated using the predicted CHF, experimental outlet quality, and an energy balance. If the absolute error was rather large, this signifies that the experimental inlet temperature was not near the triple-point and the correlation did a poor job of predicting CHF. If the error was small, then the experimental inlet temperature was only slightly higher than the triple-point and the correlation performed quite well. The present authors decided that the extra effort to account for this anomaly was not warranted since the poor performance of a correlation experiencing a multitude of these violations would be illustrated by its higher error.
6. Occasionally, an inlet conditions correlation may overpredict CHF and yield a positive outlet quality, signalling saturated fluid at the outlet, when the outlet quality is calculated using the predicted CHF, experimental inlet quality, and an energy balance. This would seem inappropriate since the correlation may only be applicable to CHF with subcooled flow at the outlet. However, the CHF trends exhibited in low-quality CHF are probably quite similar to the trends observed in subcooled CHF near saturation. Thus, a correlation based on observed parametric trends such as that developed in the present study may be able to accurately predict low-quality CHF as well as subcooled CHF. This apparent violation was also not recorded for reasons similar to those discussed in the preceding paragraph.
7. Dimensional correlations based solely on a statistical analysis of a large database [21] often predict negative CHF values even when the parameters are within the parametric range specified by the correlation. These impossible predictions were not considered when calculating the error of the correlation. However, the number of occurrences were noted for correlations in violation.
8. Mean absolute error and root-mean-square (r.m.s.) error of the correlations were calculated using

$$\text{mean absolute error} = \frac{1}{N}\sum \frac{|q_{m,\mathrm{pred}} - q_{m,\mathrm{meas}}|}{q_{m,\mathrm{meas}}} \times 100\% \tag{42}$$

and

$$\text{r.m.s. error} = \sqrt{\frac{1}{N}\sum \left(\frac{q_{m,\mathrm{pred}} - q_{m,\mathrm{meas}}}{q_{m,\mathrm{meas}}}\right)^2} \times 100\% \tag{43}$$

where N is the number of CHF data points.

6.2. *Results*

Table 5 lists the mean absolute error and r.m.s. error for each correlation when compared with CHF data from the present study and the high-CHF database. Also shown is the type of correlation (inlet or outlet conditions) and the number of adjustable constants. Adjustable constants refer to those constants which the authors manipulated in order to increase the accuracy of their correlation. Adjustable constants include those appearing in conditional statements which specify the appropriate equation from a set of equations [28, 30, 31]. The condition that a parameter such as outlet quality be either less than or greater than zero is not considered adjustable

Table 5
Performance of subcooled CHF correlations using the high-CHF database compiled in the present study

Correlation	Type	Adjustable constants	Part I [23] of present study (174 data points)		High-CHF database (1596 data points)	
			Mean absolute error (%)	r.m.s. error (%)	Mean absolute error (%)	r.m.s. error (%)
Inasaka and Nariai [27]	Outlet	9	139.3	180.1	77.4	136.4
Shah [28]	Outlet (Inlet)*	35	24.5	30.4	21.2	28.5
Caira et al. [29]	Inlet	11	22.3	31.0	21.0	31.2
Celata et al. [30]†	Outlet	8	47.1	50.0	38.2	43.4
Vandervort et al. [21]‡	Outlet	16	93.5	142.9	47.1	70.9
Caira et al. [31]§	Inlet	138	46.7	64.3	21.5	37.4
Present study						
Equation (40)	Inlet	6	22.1	33.2	17.2	24.1
Equation (39)	Outlet	5	23.8	32.4	19.1¶	25.7¶
Equation (41)	Inlet	5	17.5	22.6	15.1	19.5

* Consists of two sets of equations (one based on outlet quality and the other on inlet quality) and conditional statements for choosing the appropriate set. Only five data points in the high-CHF database required the correlation based on inlet quality.
† Two of eight adjustable constants are applicable only to saturated outlet conditions.
‡ Predicted negative CHF values for 53 data points.
§ Correct constants were obtained from Caruso [36].
¶ Near-saturated CHF data ($x_o > -0.05$) were excluded (233 data points).

[28, 30]. The exponent of a parameter in a polynomial function is also not considered adjustable [27].

Figure 8 compares CHF data from the high-CHF database with CHF predicted by each of the six previously published correlations. The usefulness of a correlation as a predictive tool for subcooled high-CHF can be determined by examining the relative data density inside or outside of the $\pm 40\%$ error band. The Inasaka and Nariai [27] and Vandervort et al. [21] correlations are obviously poor with a large fraction of data being severely overpredicted or both over and underpredicted, respectively. The Celata et al. [30] and Caira et al. [31] correlations generally underpredict or overpredict CHF, respectively; also, the error is larger when predicting CHF for data from Part I [23] of the present study, indicating that these correlations may only be adequate over a limited parametric range. Furthermore, Caira et al. [31] attempted to improve the accuracy of their earlier correlation [29] by increasing the number of adjustable constants from 11 to 138. The forms of the correlations were identical except that a different set of eleven constants was utilized within different regions of mass velocity and pressure. The new correlation by Caira et al. [31] resulted in nearly the same mean absolute error as their prior correlation for the high-CHF data but resulted in an r.m.s. error 20% higher. Visual observation of Fig. 8 clearly shows that their earlier correlation performs better, indicating that r.m.s. error is probably a better means for determining the predictive capabilities of a correlation. The larger errors of the new correlation resulted from a combination of a large number of adjustable constants (138) and a limited number of data points within some regions (e.g., only eight data points in the region $G > 20\,000$ kg m^{-2} s^{-1} and $3 < P < 5$ bars were available to obtain eleven constants, which is statistically impossible to accomplish). Only the correlations of Shah [28] and Caira et al. [29] appear to be moderately acceptable for predicting subcooled high-CHF.

Figure 9(a) and (b) compare the CHF data with CHF predicted by the inlet and outlet conditions correlations, which were developed on the basis of equations (24) and (25), respectively, and the parametric trends observed in a subset of the high-CHF database. The graphs on the left-hand side show only the 174 CHF data points from Part I [23], while the graphs on the right-hand side show the entire high-CHF database (1596 data points). Figure 10 shows the assessment of the superior, inlet conditions correlation, which was formulated from the outlet conditions correlation using an energy balance. In all cases, the inlet conditions correlation shown in Fig. 10 had the lowest mean absolute and r.m.s. error, with 96% of the high-CHF database predicted within $\pm 40\%$. The average of the ratio of predicted-to-measured CHF was 0.985 (not listed in Table 5) meaning this correlation is only slightly more likely to underpredict CHF than it is to overpredict CHF. Both inlet conditions correlations, shown in Figs 9(a) and 10, had lower mean absolute and r.m.s. errors than the previously published correlations. The correlation in Fig. 9(a) overpredicted CHF and yielded a positive outlet quality for only 3.2% of the

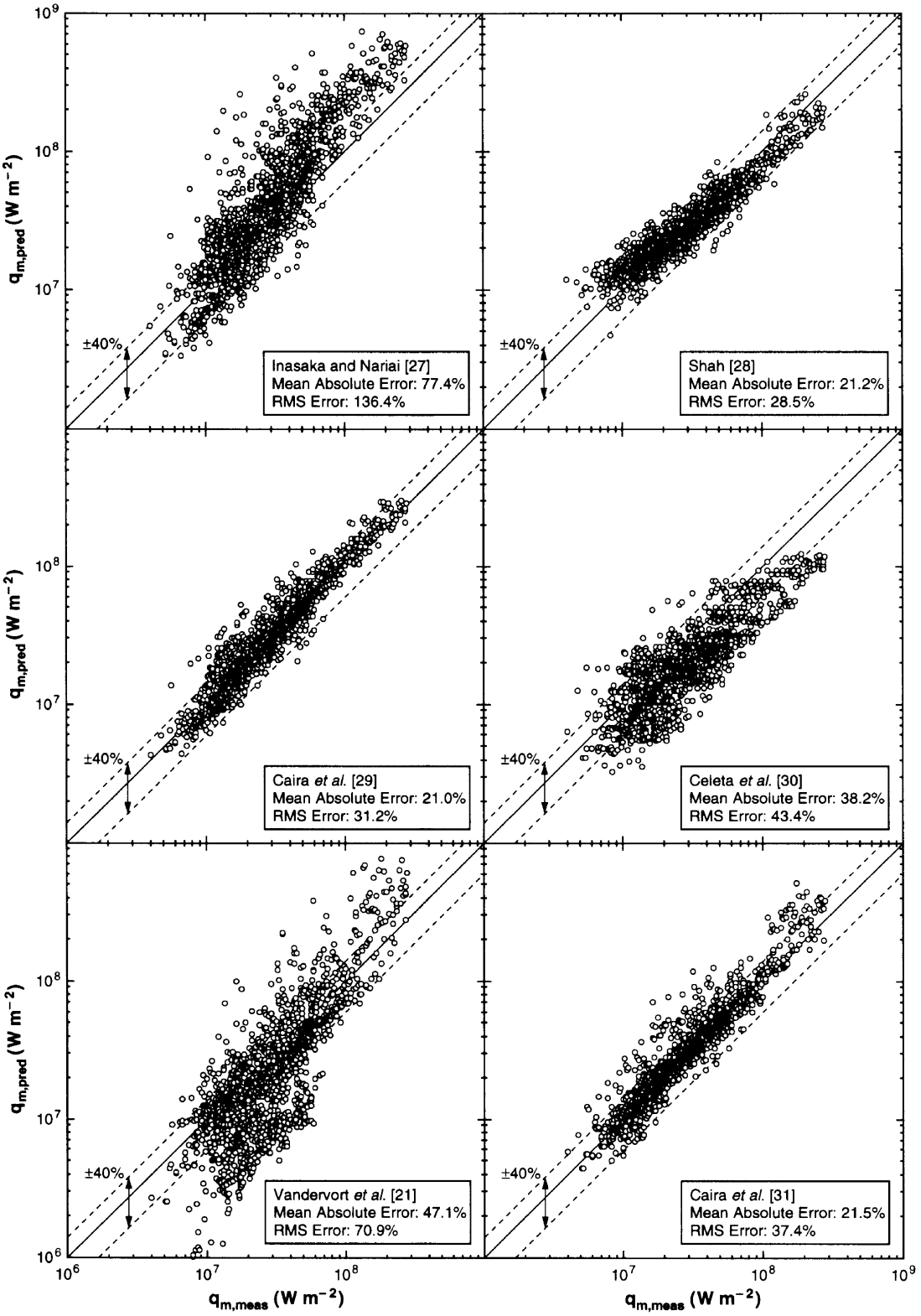

Fig. 8. Assessment of several well-known CHF correlations applicable to high-CHF using the high-CHF database.

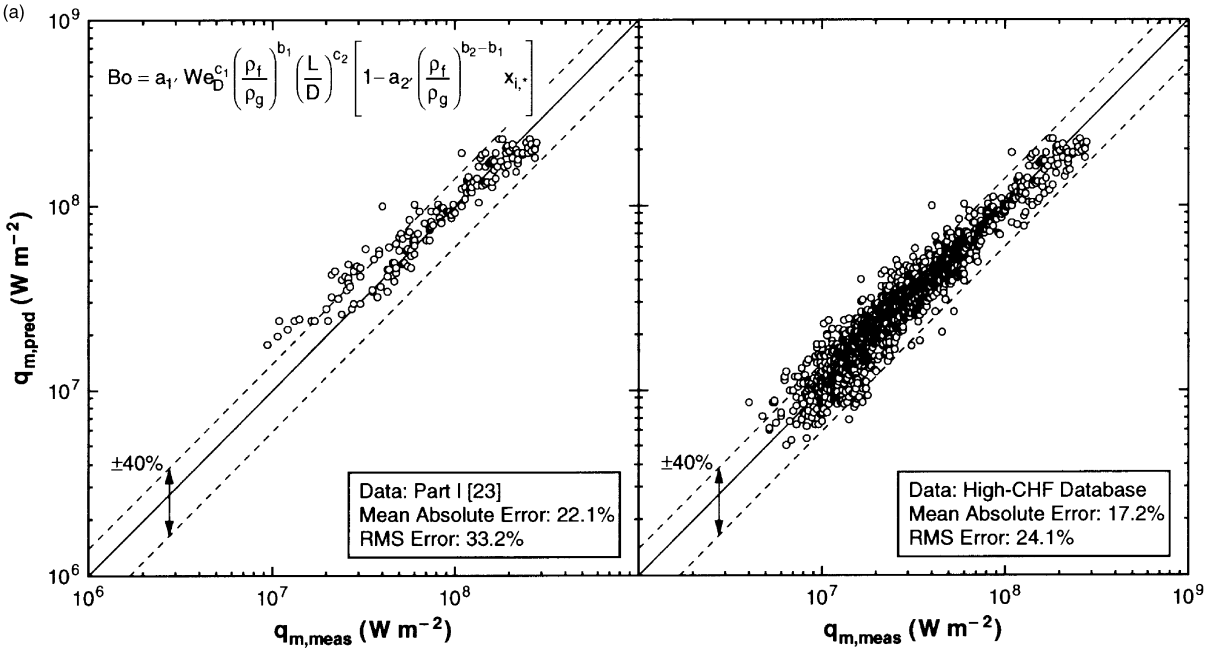

(b)

	Outlet Quality	CHF Data Points	Mean Absolute Error	RMS Error
○	$x_o \leq -0.05$	1363	19.1	25.7
□	$-0.05 < x_o < 0$	233	52.5	56.3
○ □	$x_o \leq 0$	1596	24.0	32.1

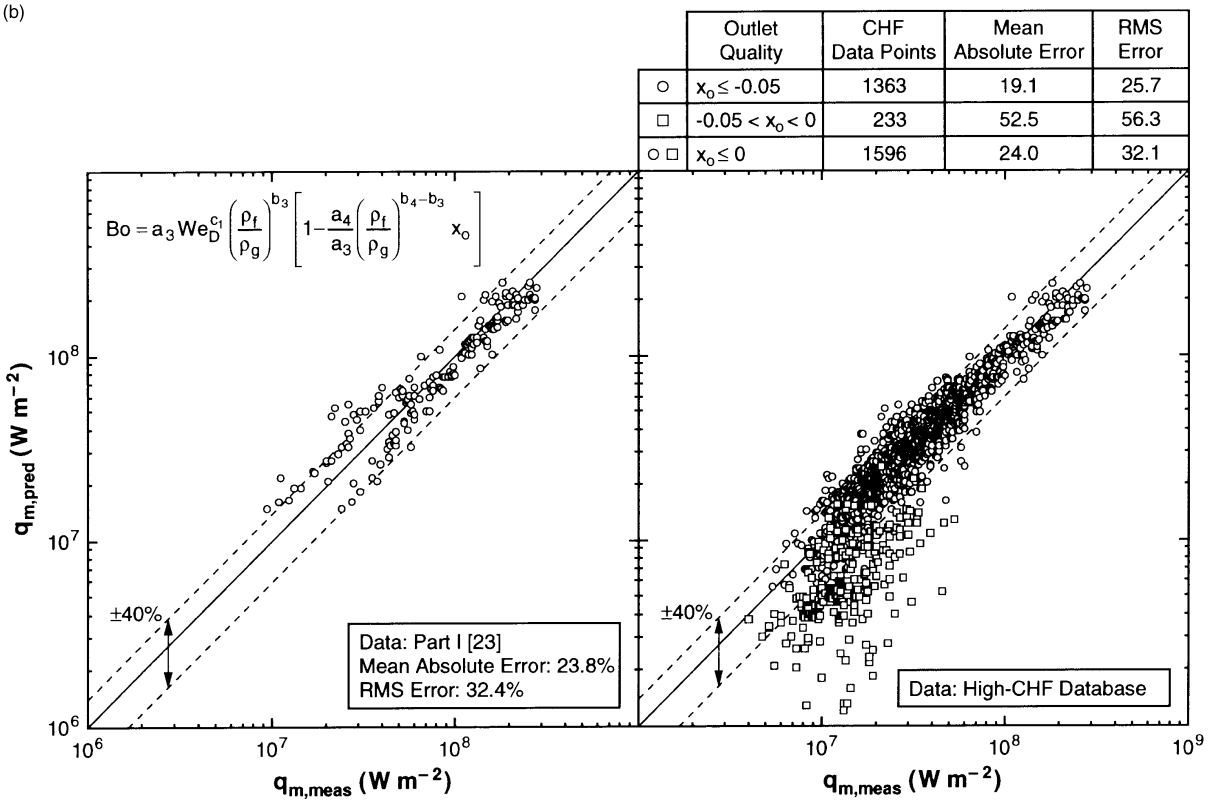

Fig. 9. Assessment of the (a) inlet and (b) outlet conditions, subcooled CHF correlations using CHF data from Part I [23] of the present study and the high-CHF database.

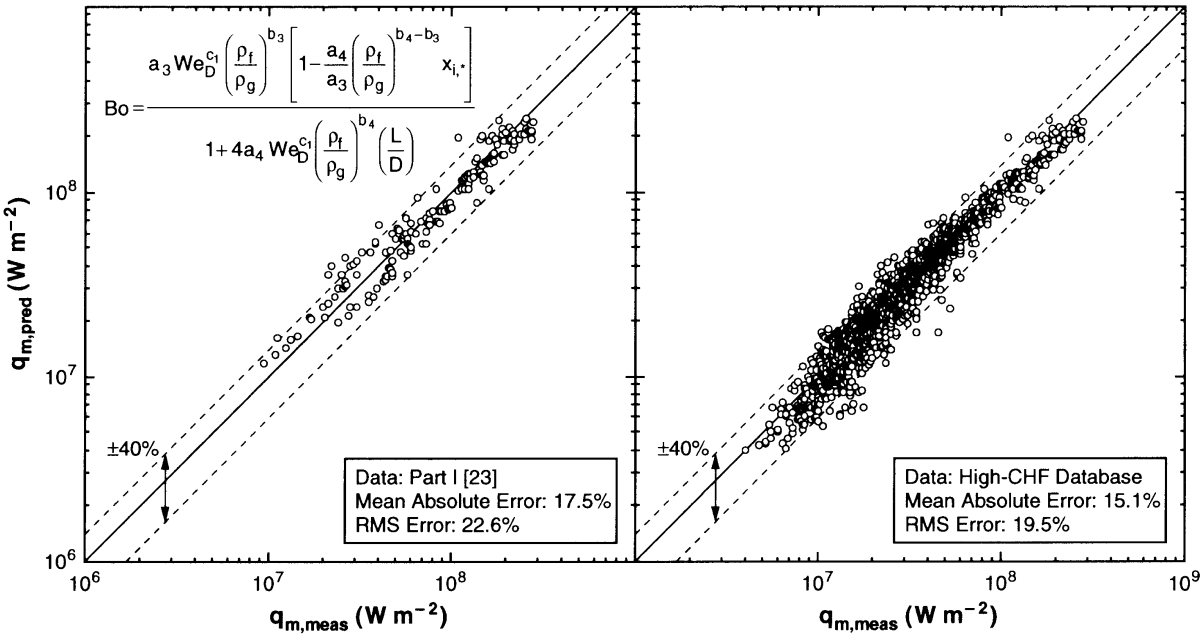

Fig. 10. Assessment of the superior, inlet conditions, subcooled CHF correlation which was formulated from the outlet conditions correlation using an energy balance.

high-CHF database. On the other hand, the correlation in Fig. 10 did not overpredict any of the data enough to produce a positive outlet quality.

The outlet conditions correlation shown in Fig. 9(b) predicted 80% of the entire high-CHF database within $\pm 40\%$. This correlation overpredicted CHF and yielded an inlet temperature below the triple-point temperature for 2.6% of the high-CHF database. Of the 209 CHF data points underpredicted by more than 40%, over 86% had an experimental outlet quality greater than -0.05 with most of these having an outlet pressure below 10 bars. When data with an outlet quality above -0.05 were excluded (representing only 15% of the high-CHF database), the mean absolute and r.m.s. errors were both reduced by 20% from their values with the entire high-CHF database. These errors are lower than those of the previously published correlations. Transforming the outlet conditions correlation in to an inlet conditions correlation using an energy balance (and without altering any of the constants) remarkably lowered the mean absolute and r.m.s. errors by 37.1 and 39.3%, respectively, by predicting the near-saturated CHF data with better accuracy. Since the correlations developed in the present study were based only on observed parametric trends, the larger errors associated with the outlet conditions correlation for near-saturated CHF data may indicate a CHF trigger mechanism different from that characteristic of highly-subcooled CHF. No attempt was made to increase the accuracy of the correlations by adjusting the coefficients using nonlinear regression. The superiority of all correlations developed in the present study was obtained solely by methodically examining a subset of the high-CHF database.

7. Supplemental discussion

7.1. *Nonuniform axial heat flux profile*

While an inlet conditions (also known as upstream or non-local) correlation depends upon the axial heat flux profile (uniform in the present study) and heated length, an outlet (also known as local) conditions correlation depends solely upon the flow conditions at the location of burnout (outlet of a uniformly heated tube in the present study). Thus, of the correlations developed in the present study, only the outlet (local) conditions correlation is well suited for predicting CHF in tubes having a nonuniform axial heat flux profile such as the sinusoidal profile,

$$q(z) = q_{max}\sin(\pi z/L), \tag{44}$$

often found in nuclear reactor fuel elements [57]. In this case, CHF occurs upstream and both the location and magnitude of CHF can be predicted by a local conditions correlation. An energy balance from the inlet to a downstream location, z, yields an equation for the local enthalpy,

$$h(z) = h_i + \frac{4}{DG}\int_0^z q(z)\,dz. \quad (45)$$

A pressure drop model such as that developed in the present study is then required in order to calculate the local thermodynamic equilibrium quality from the local enthalpy given by equation (45) and the local pressure. A local conditions correlation predicts CHF to occur at location z when the local quality and heat flux related by equation (45) and the pressure drop model also satisfy the CHF correlation. For a complex axial heat flux distribution, CHF may have already occurred downstream. Thus, in order to predict the first occurrence of CHF anywhere in the tube, the shape of the profile must be assumed, the total power incrementally increased, and the above calculation conducted at incremental streamwise locations beginning from the inlet.

The outlet (local) conditions, subcooled CHF correlation developed in the present study, which is only valid for a local quality below -0.05, should be validated with CHF data obtained with a nonuniform axial heat flux profile. For a uniform axial heat flux profile, the outlet conditions correlation is quite superior to the others, having mean absolute and r.m.s. errors nearly half that of the values for the other correlations [21, 27, 30] based on outlet conditions. Note that Shah's [28] outlet conditions correlation is not a true local conditions correlation since CHF depends upon heated length when $L/D < 50$ and, thus, the correlation is applicable only to uniformly heated tubes.

7.2. Effect of pressure on CHF

None of the data in the high-CHF database were obtained by systematically varying the pressure while maintaining either a constant inlet or outlet quality. Therefore, the effect of pressure on CHF could only be ascertained by examining a correlation with proven accuracy. The inlet conditions correlation developed in the present study, equation (41), was evaluated from atmospheric pressure to the critical pressure for $D = 2$ mm, $L/D = 20$, $G = 5000\ \mathrm{kg\,m^{-2}\,s^{-1}}$ (typical of the high-CHF database) with either constant inlet temperature, inlet quality, or outlet quality. Evaluating the inlet conditions correlation at constant outlet quality is equivalent to evaluating the outlet conditions correlation, equation (39), since the two correlations are related by an energy balance.

The curves in Fig. 11(a) obtained at several inlet temperatures agree with the experimental trends in Fig. 14 from Part I [23], which show a lower CHF near atmospheric pressure and a relatively smaller effect of pressure on CHF at higher pressures (below 170 bars). The upper and lower boundaries represent an inlet temperature equal to the triple-point temperature and an outlet quality equal to zero, respectively. The first condition is impossible to violate, while violating the second condition simply means that the fluid is saturated at the outlet. As the pressure approaches the critical pressure, CHF drastically decreases. These trends for a constant inlet temperature have been widely reported in the CHF literature.

Figure 11(b) shows that CHF continually decreases with increasing pressure for a constant inlet quality below approximately -0.2. Near an inlet quality of -0.1, CHF initially decreases with increasing pressure until 10–20 bars, at which point, CHF becomes somewhat unaffected by pressure and, then, again decreases with increasing pressure from 150 bars to the critical pressure. For near-saturated inlet qualities, CHF actually increases slightly with increasing pressure until the outlet becomes saturated, at which point, the correlations can no longer be utilized with confidence. CHF decreases linearly with increasing pressure for a highly subcooled inlet ($x_i < -1.0$).

The curves in Fig. 11(c) obtained at several outlet qualities exhibit trends similar to those observed in Fig. 11(b), which is expected since inlet and outlet quality are linearly related by an energy balance. Recall that the outlet conditions correlation seemed to be invalid for near-saturated conditions ($x_o > -0.05$), especially at low pressures ($P < 10$ bars). In this region, the correlation predicts an increase in CHF with increasing pressure, whereas the curve for $x_o = -0.05$ (and also -1.0) shows a step decrease, but at much higher CHF values. The correlation underpredicts the CHF data in this near-saturated region meaning that the actual curve for $x_o = -0.02$ should be much closer to and exhibit the trends of the curve for $x_o = -0.05$. Thus, it can be concluded that the outlet conditions correlation should not be used for $x_o > -0.05$ without further investigation of near-saturated, low-pressure CHF.

8. Conclusions

Subcooled high-CHF data for water flow in a uniformly heated tube were compiled from the world literature dating back to 1949. The database was filtered for duplicate and unreliable data. A pressure drop model applicable to subcooled flow boiling in tubes with inlet and outlet plenums was developed in order to determine the pressure at the burnout location (i.e., end of the heated length), an important parameter required by CHF correlations. Several well-known subcooled CHF correlations applicable to the high mass velocities required to achieve high-CHF values were analyzed using this database. Simple, dimensionless, subcooled CHF correlations based on inlet conditions (valid for $x_o \leqslant 0$) and outlet conditions (valid only for $x_o \leqslant -0.05$) were developed by carefully observing parametric trends in CHF data from Ornatskii and Kichigin [3, 5], Ornatskii

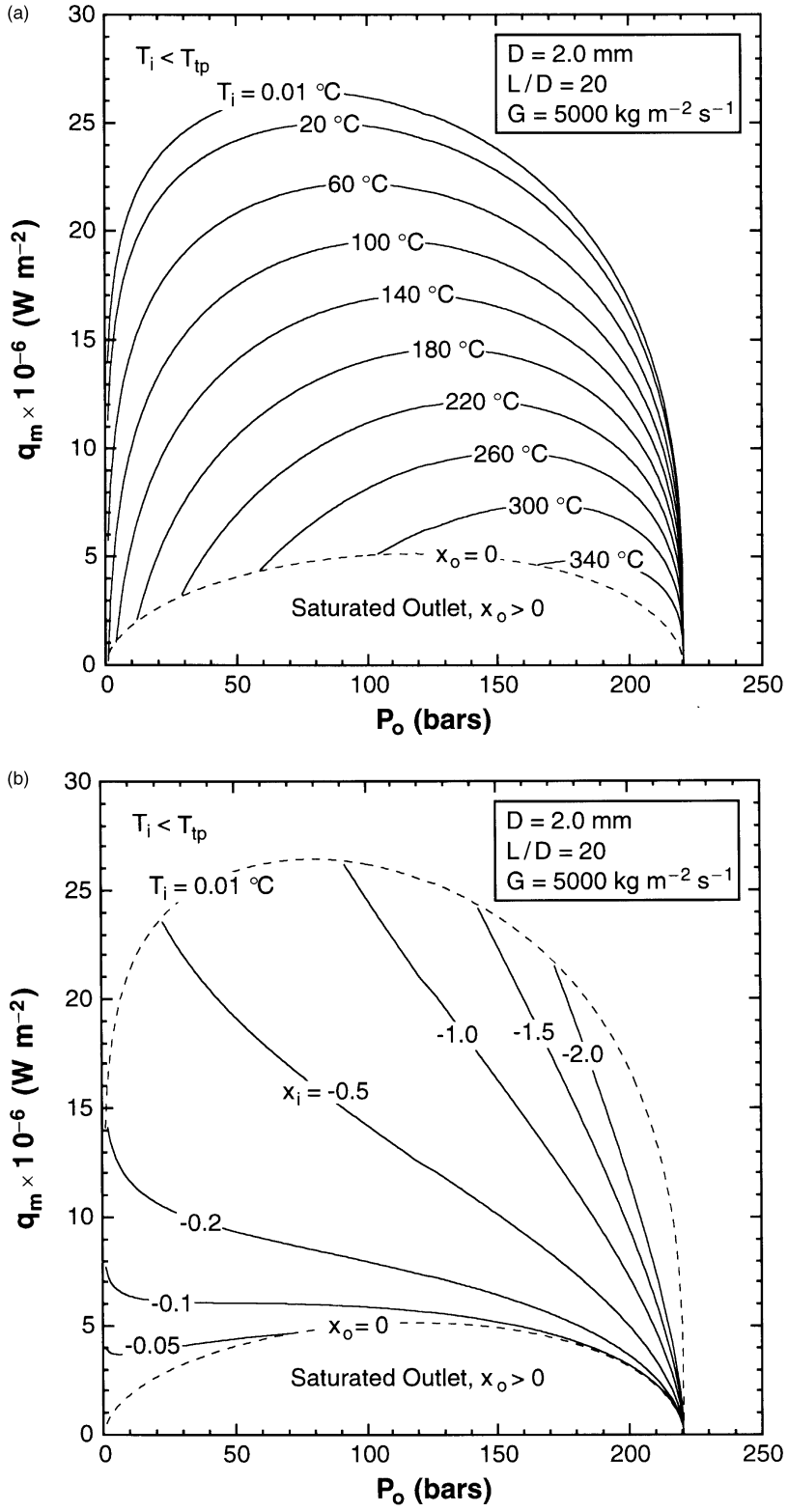

Fig. 11. Effect of pressure on CHF for constant (a) inlet temperature, (b) inlet quality, and (c) outlet quality evaluated using the inlet conditions correlation developed in the present study, equation (41).

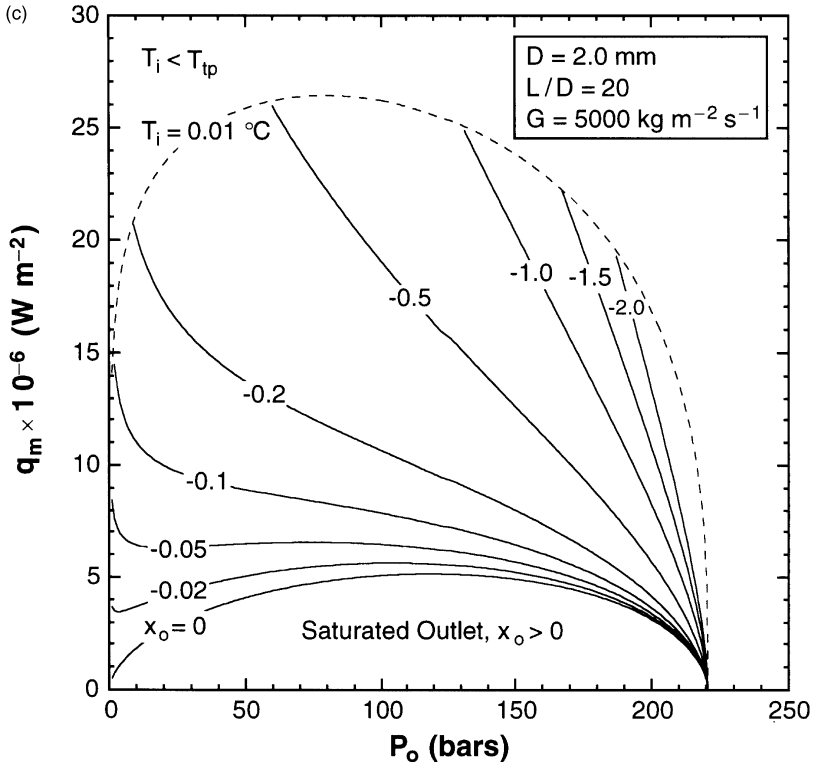

Fig. 11. *Continued.*

[7], and Part I [23] of the present study. Both the outlet conditions correlation (equation (39)) and the inlet conditions correlation (equation (41)), which was formulated from the outlet conditions correlation using an energy balance, contain only five adjustable constants in contrast to the large number of constants required by the other correlations. Although these new correlations were developed by observing the trends in a subset of the high-CHF database (447 data points) and not nonlinear regression with the entire database, they were quite superior to the previously published correlations, which were mostly based on statistical analyses of large databases. The mean absolute and r.m.s. errors for equation (41) were 15.1 and 19.5%, respectively, 29 and 32% less than the next most accurate correlation. The authors recommend this inlet conditions correlation (shown in Table 4) for the prediction of subcooled CHF with water flow in a uniformly heated tube and for the design of high-flux cooling schemes for conditions within the parametric range of the high-CHF database.

Acknowledgements

The authors are grateful for the support of the Office of Basic Energy Sciences of the U.S. Department of Energy (Grant No. DE-FG02-93ER14394.A003). Financial support for the first author was provided in the form of the Link Foundation Energy Fellowship and the Ingersoll-Rand Fellowship.

References

[1] W.R. Gambill, N.D. Greene, Boiling burnout with water in vortex flow, Chemical Engineering Progress 54 (10) (1958) 68–76.

[2] W.R. Gambill, R.D. Bundy, R.W. Wansbrough, Heat transfer, burnout, and pressure drop for water in swirl flow through tubes with internal twisted tapes, Chemical Engineering Progress Symposium Series No. 32 57 (1961) 127–137. ORNL-2911, Oak Ridge National Laboratory, Oak Ridge, TN.

[3] A.P. Ornatskii, A.M. Kichigan, An investigation of the dependence of critical thermal loading on weight velocity, underheating and pressure, Teploenergetika 8 (2) (1961) 75–79.

[4] A.E. Bergles, W.M. Rohsenow, Forced-convection surface-boiling heat transfer and burnout in tubes of small diameter, NP-11831, U.S. Atomic Energy Commission, 1962, DSR Report 8767-21, Massachusetts Institute of Technology, Cambridge, MA.

[5] A.P. Ornatskii, A.M. Kichigan, Critical heat loads in high-

pressure boiling of underheated water in small diameter tubes, Teploenergetika 9 (6) (1962) 44–47. ORNL-tr-107, Oak Ridge National Laboratory, Oak Ridge, TN.

[6] A.E. Bergles, Subcooled burnout in tubes of small diameter, ASME Paper No. 63-WA-182, 1963.

[7] A.P. Ornatskii, Critical heat loads and heat transfer for a forced flow of water in tubes in the region of superhigh pressures (175–220 atm), Teploenergetika 10 (3) (1963) 66–69. AEC-tr-6401, U.S. Atomic Energy Commission.

[8] J. Mayersak, S.D. Raezer, E.A. Bunt, Confirmation of Gambill-Green straight-flow burnout heat flux equation at higher flow velocity, ASME Journal of Heat Transfer 86 (1964) 297–298.

[9] A.P. Ornatskii, L.S. Vinyarskii, Heat transfer crisis in a forced flow of underheated water in small-bore tubes, Teplofizika Vysokikh Temperatur 3 (1965) 444–451; High Temperature 3 (1965) 400–406.

[10] B.C. Skinner, C.S. Loosmore, Subcooled critical heat flux for water in round tube, M.S. thesis, Massachusetts Institute of Technology, Cambridge, MA, 1965.

[11] Yu.A. Zeigarnik, N.P. Privalov, A.I. Klimov, Critical heat flux with boiling of subcooled water in rectangular channels with one-sided supply of heat, Teploenergetika 28 (1) (1981) 48–51; Thermal Engineering 28 (1981) 40–43.

[12] H. Nariai, F. Inasaka, T. Shimura, Critical heat flux of subcooled flow boiling in narrow tube, in: P.J. Marto, I. Tanasawa (Eds), Proceedings of the 1987 ASME–JSME Thermal Engineering Joint Conference, vol. 5, American Society of Mechanical Engineers, New York, 1987, pp. 455–462.

[13] R.D. Boyd, Subcooled water flow boiling experiments under uniform high heat flux conditions, Fusion Technology 13 (1988) 131–142.

[14] R.D. Boyd, Subcooled water flow boiling at 1.66 MPa under uniform high heat flux conditions, Fusion Technology 16 (1989) 324–330.

[15] F. Inasaka, H. Nariai, Critical heat flux of subcooled flow boiling with water, in: U. Müller, K. Rehme, K. Rust (Eds), Proceedings of the Fourth International Topical Meeting on Nuclear Reactor Thermal-Hydraulics: NURETH-4, vol. 1, G. Braun, Karlsruhe, Germany, 1989, pp. 115–120.

[16] G.P. Celata, M. Cumo, A. Mariani, CHF in highly subcooled flow boiling with and without turbulence promoters, European Two-Phase Flow Group Meeting, Stockholm, Sweden, 1–3 June, 1992, Paper C1.

[17] G.P. Celata, M. Cumo, A. Mariani, Subcooled water flow boiling CHF with very high heat fluxes, Revue Générale de Thermique 31 (1992) 106–114.

[18] G.P. Celata, M. Cumo, A. Mariani, Burnout in highly subcooled water flow boiling in small diameter tubes, International Journal of Heat and Mass Transfer 36 (1993) 1269–1285.

[19] G.P. Celata, A. Mariani, A data set of critical heat flux in water subcooled flow boiling, Personal Communication, ENEA Casaccia, Rome, Italy, April 2, 1993. Addendum to Specialists' Workshop on the Thermal-Hydraulics of High Heat Flux Components in Fusion Reactors, Rome, Italy, 9–11 September, 1992.

[20] G.P. Gaspari, G. Cattadori, Subcooled flow boiling burnout in tubes with and without turbulence promoters, Experimental Thermal and Fluid Science 8 (1994) 28–34.

[21] C.L. Vandervort, A.E. Bergles, M.K. Jensen, An experimental study of critical heat flux in very high heat flux subcooled boiling, International Journal of Heat and Mass Transfer 37 (Suppl. 1) (1994) 161–173.

[22] G.P. Celata, Personal Communication, ENEA Casaccia, Rome, Italy, 24 October 1996 and 8 November 1996.

[23] I. Mudawar, M.B. Bowers, Ultra-high critical heat flux (CHF) for subcooled water flow boiling—I: CHF data and parametric effects for small diameter tubes, International Journal of Heat and Mass Transfer 42 (1999) 1405–1428.

[24] F. Inasaka, Critical heat flux of subcooled flow boiling in water under uniform heating conditions, Papers of Ship Research Institute 30 (4) (1993) 1–69.

[25] D.D. Hall, I. Mudawar, Critical heat flux (CHF) for water flow in tubes. Volume I. Compilation and assessment of world CHF data, Purdue University, Boiling and Two-Phase Flow Laboratory, West Lafayette, IN, 1998.

[26] T.F. Irvine Jr, P.E. Liley, Steam and Gas Tables with Computer Equations, Academic Press, Orlando, FL, 1984, pp. 21–23.

[27] F. Inasaka, H. Nariai, Critical heat flux and flow characteristics of subcooled flow boiling in narrow tubes, JSME International Journal 30 (1987) 1595–1600.

[28] M.M. Shah, Improved general correlation for critical heat flux during upflow in uniformly heated vertical tubes, International Journal of Heat and Fluid Flow 8 (1987) 326–335.

[29] M. Caira, G. Caruso, A. Naviglio, Requirements of high heat flux for fusion reactor components: revised models and correlations predict critical heat flux in subcooled flow boiling, ANS Proceedings: 1993 National Heat Transfer Conference, American Nuclear Society, La Grange, IL, 1993, pp. 383–390.

[30] G.P. Celata, M. Cumo, A. Mariani, Assessment of correlations and models for the prediction of CHF in water subcooled flow boiling, International Journal of Heat and Mass Transfer 37 (1994) 237–255.

[31] M. Caira, G. Caruso, A. Naviglio, A correlation to predict CHF in subcooled flow boiling, International Communications in Heat and Mass Transfer 22 (1995) 35–45.

[32] L.S. Tong, Boundary-layer analysis of the flow boiling crisis, International Journal of Heat and Mass Transfer 11 (1968) 1208–1211.

[33] S.S. Kutateladze, A.I. Leont'ev, Some applications of the asymptotic theory of the turbulent boundary layer, Proceedings of the Third International Heat Transfer Conference, vol. 3, American Institute of Chemical Engineers, New York, 1966, pp. 1–6.

[34] F. Inasaka, H. Nariai, Critical heat flux of subcooled flow boiling for water in uniformly heated straight tubes, Fusion Engineering and Design 19 (1992) 329–337.

[35] R.W. Bowring, A simple but accurate round tube, uniform heat flux, dryout correlation over the pressure range 0.7–17 MN/m^2 (100–2500 psia), AEEW-R 789, United Kingdom Atomic Energy Authority, Atomic Energy Establishment, Winfrith, United Kingdom, 1972.

[36] G. Caruso, Personal Communication, University of Rome "La Sapienza", Department of Nuclear Engineering and Energy Conversion, Rome, Italy, 26 February 1996.

[37] M.M. Shah, A generalized graphical method for predicting CHF in uniformly heated vertical tubes, International Journal of Heat and Mass Transfer 22 (1979) 557–568.

[38] D.D. Hall, I. Mudawar, Critical heat flux (CHF) for water flow in tubes. Volume III. Subcooled CHF correlations, Purdue University, Boiling and Two-Phase Flow Laboratory, West Lafayette, IN, 1998.
[39] R.G. Deissler, Analysis of turbulent heat transfer and flow in the entrance regions of smooth passages, NACA TN 3016, National Advisory Committee for Aeronautics, Washington, DC, 1953.
[40] R.J. Phillips, L.R. Glicksman, R. Larson, Forced-convection, liquid-cooled, microchannel heat sinks for high-power-density microelectronics, in: W. Aung (Ed.), Cooling Technology for Electronic Equipment, Hemisphere Pub. Corp., New York, 1988, pp. 295–316.
[41] W.M. Kays, Loss coefficients for abrupt changes in flow cross section with low Reynolds number flow in single and multiple-tube systems, Transactions of ASME 72 (1950) 1067–1074.
[42] J. Weisbach, Die Experimental-Hydraulik, J.S. Engelhardt, Freiberg, Germany, 1855, p. 133.
[43] R.P. Benedict, N.A. Carlucci, S.D. Swetz, Flow losses in abrupt enlargements and contractions, ASME Journal of Engineering for Power 88 (1966) 73–81.
[44] M.S. Bhatti, R.K. Shah, Turbulent and transition flow convective heat transfer in ducts, in: S. Kakaç, R.K. Shah, W. Aung (Eds), Handbook of Single-Phase Convective Heat Transfer, John Wiley and Sons, New York, 1987, Chap. 4.
[45] U. Grigull, J. Straub, P. Schiebener, Steam Tables in SI-Units, 3rd ed., Springer-Verlag, Berlin, Germany, 1990, pp. 78–85.
[46] L. Haar, J.S. Gallagher, G.S. Kell, NBS/NRC Steam Tables, Hemisphere Pub. Corp., Washington, DC, 1984, pp. 267, 316.
[47] D.D. Hall, I. Mudawar, Evaluation of subcooled critical heat flux correlations using the PU-BTPFL CHf database for vertical upflow of water in a uniformly heated round tube, Nuclear Technology 117 (1997) 234–247.
[48] M.E. Nissley, A.J. Friedland, R.P. Knott, Considerations for comparing CHF correlations, in: H. Kakihana, N. Todreas, Y.Y. Hsu, R. Kiyose, J. Wakabayashi, C. Chiu, H. Nariai, T. Kobori, A. Inoue, J. Chao (Eds), Proceedings of Second International Topical Meeting on Nuclear Power Plant Thermal Hydraulics and Operations, Atomic Energy Society of Japan, Tokyo, Japan, 1986, pp. 9–13.
[49] F. Inasaka, H. Nariai, Evaluation of subcooled critical heat flux correlations for tubes with and without internal twisted tapes, Proceedings of the Fifth International Topical Meeting on Reactor Thermal Hydraulics: NURETH-5, vol. 4, American Nuclear Society, La Grange, IL, 1992, pp. 919–928.
[50] P. Bricard, A. Souyri, Understanding and modelling DNB in forced convective boiling: a critical review, in: G.P. Celata, R.K. Shah (Eds), Two-Phase Flow Modelling and Experimentation 1995, vol. 2, Edizioni ETS, Pisa, Italy, 1995, pp. 843–851.
[51] G.P. Celata, On the application method of critical heat flux correlations, Nuclear Engineering and Design 163 (1996) 241–242.
[52] D.C. Groeneveld, On the definition of critical heat flux margin, Nuclear Engineering and Design 163 (1996) 245–247.
[53] P. Hejzlar, N.E. Todreas, Consideration of critical heat flux margin prediction by subcooled or low quality critical heat flux correlations, Nuclear Engineering and Design 163 (1996) 215–223.
[54] P. Hejzlar, N.E. Todreas, Response to contributors' letters and technical notes, Nuclear Engineering and Design 163 (1996) 273–279.
[55] F. Inasaka, H. Nariai, Evaluation of subcooled critical heat flux correlations for tubes with and without internal twisted tapes, Nuclear Engineering and Design 163 (1996) 225–239.
[56] M. Siman-Tov, Application of energy balance and direct substitution methods for thermal margins and data evaluation, Nuclear Engineering and Design 163 (1996) 249–258.
[57] J.G. Collier, J.R. Thome, Convective Boiling and Condensation, 3rd ed., Clarendon Press, Oxford, United Kingdom, 1994, pp. 375–380.